cytes. While most of these individual PF compounds showed antagonistic effects or almost no effect on GIRK channels, only PF 419 showed an apparent agonistic effect on both GIRK1/2 and GIRK1/4 cannels (Fig. **2a, b**). Therefore, PF 419 was selected as a candidate agonist. In addition, PF 40, PF 236, and PF 246, which induced comparatively higher percentage inhibition of GIRK currents, were selected as candidate antagonists (Fig. **2b**).

In the third screening step, the four PF compounds selected above (PF 419, PF 40, PF 236, PF 246) were applied to the oocytes expressing the GIRK1/2 channel ($n$ = 5) and GIRK1/4 channel ($n$ = 5) at various concentrations. Considering the results in our preliminary experiments testing the effect of each compound at 0.1, 1, and 10 μM (data not shown), the concentrations of each compound to examine the concentration-response relationships were set at 1, 3, 10, 30, and 100 μM. Fig. (**3**) represents the concentration-response relationships for each PF compound. PF 419 activated GIRK currents dose-dependently, whereas PF 40, PF 236, and PF 246 inhibited them dose-dependently. Two-way ANOVA revealed that there were significant main effects of the concentrations of PF compounds on the current responses to PF 419 ($F_{4,40}$ = 8.606, $P$ < 0.001), PF 40 ($F_{4,40}$ = 75.475, $P$ < 0.001), PF 236 ($F_{4,40}$ = 80.160, $P$ < 0.001), and PF 246 ($F_{4,40}$ = 227.702, $P$ < 0.001). There were significant main effects of the GIRK subunit compositions on the current responses in PF 419 ($F_{1,40}$ = 6.078, $P$ = 0.018), PF 40 ($F_{1,40}$ = 19.865, $P$ < 0.001), and PF 236 ($F_{1,40}$ = 50.590, $P$ < 0.001). Significant interactions were observed between the concentrations and GIRK subunit compositions in PF 40 ($F_{4,40}$ = 3.252, $P$ = 0.021) and PF 236 ($F_{4,40}$ = 4.371, $P$ = 0.005). *Post hoc* analysis revealed a significant difference between the GIRK1/2 and GIRK1/4 channels at 100 μM ($P$ = 0.004) in PF 419, at 30 μM ($P$ = 0.004) and 100 μM ($P$ < 0.001) in PF 40, and at 10 μM ($P$ = 0.001), 30 μM ($P$ < 0.001), and 100 μM ($P$ < 0.001) in PF 236 (Fig. **3**). Inhibition concentration ($IC_{50}$) values were calculated for PF 40, PF 236, and PF 246 (Table **1**). In addition, we examined the selectivity of these compounds for GIRK channels by applying them to oocytes expressing the IRK2 channel ($n$ = 2). All four compounds showed almost no or negligible effects on IRK2 channels (data not shown), suggesting that these compounds were selective for GIRK channels.

## DISCUSSION

In the first step of the screening process, most pools of PF compounds showed apparent antagonistic effects and a few showed agonistic effects on GIRK channels, possibly because the PF compounds used in the present assay were selected from the fluoxetine derivatives that are known to inhibit GIRK channels [22]. However, several pools of PF compounds exhibited almost no effects on GIRK channels. It

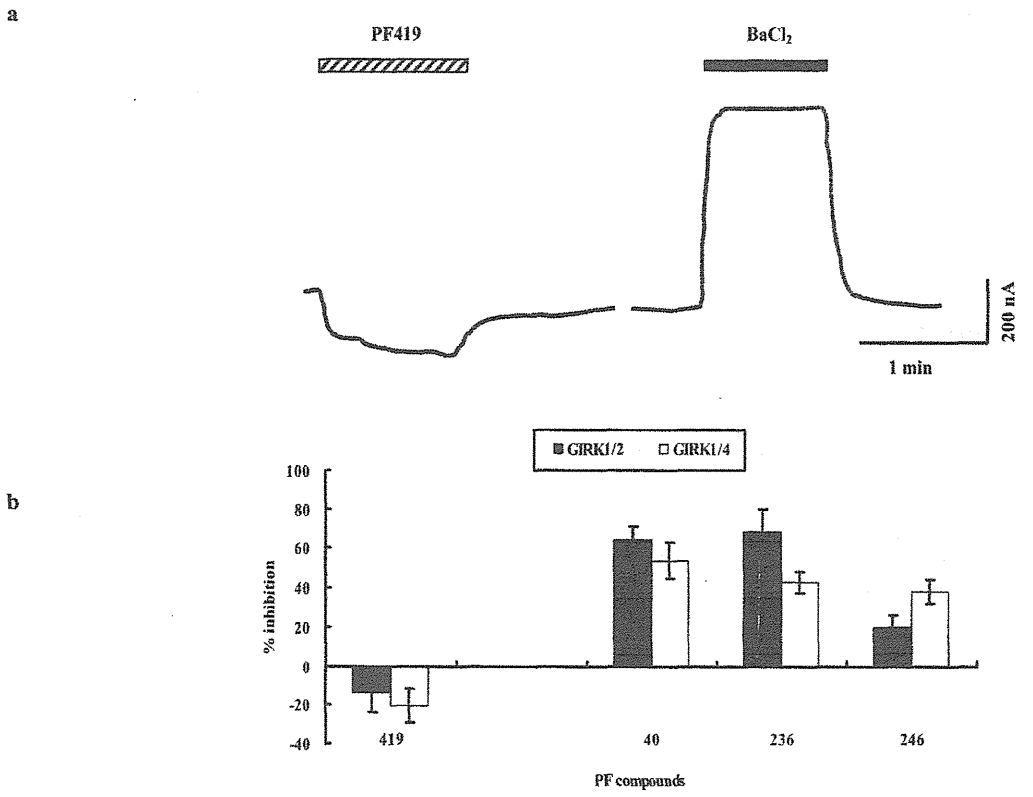


**Fig. (2). Candidate Agonist and Antagonists Identified in the Second Screening Step.** PF 419 was selected as a candidate agonist, and PF 40, PF 236, and PF 246 were selected as candidate antagonists in the second screening step. **a**. Traces of typical current responses to PF 419 (30 μM) and $BaCl_2$ (2 mM) in the oocyte expressing the GIRK1/4 channel. The striped and filled bars represent the duration of the application of PF 419 and $BaCl_2$, respectively. **b**. The normalized current responses to the selected PF compounds by the response to $BaCl_2$.

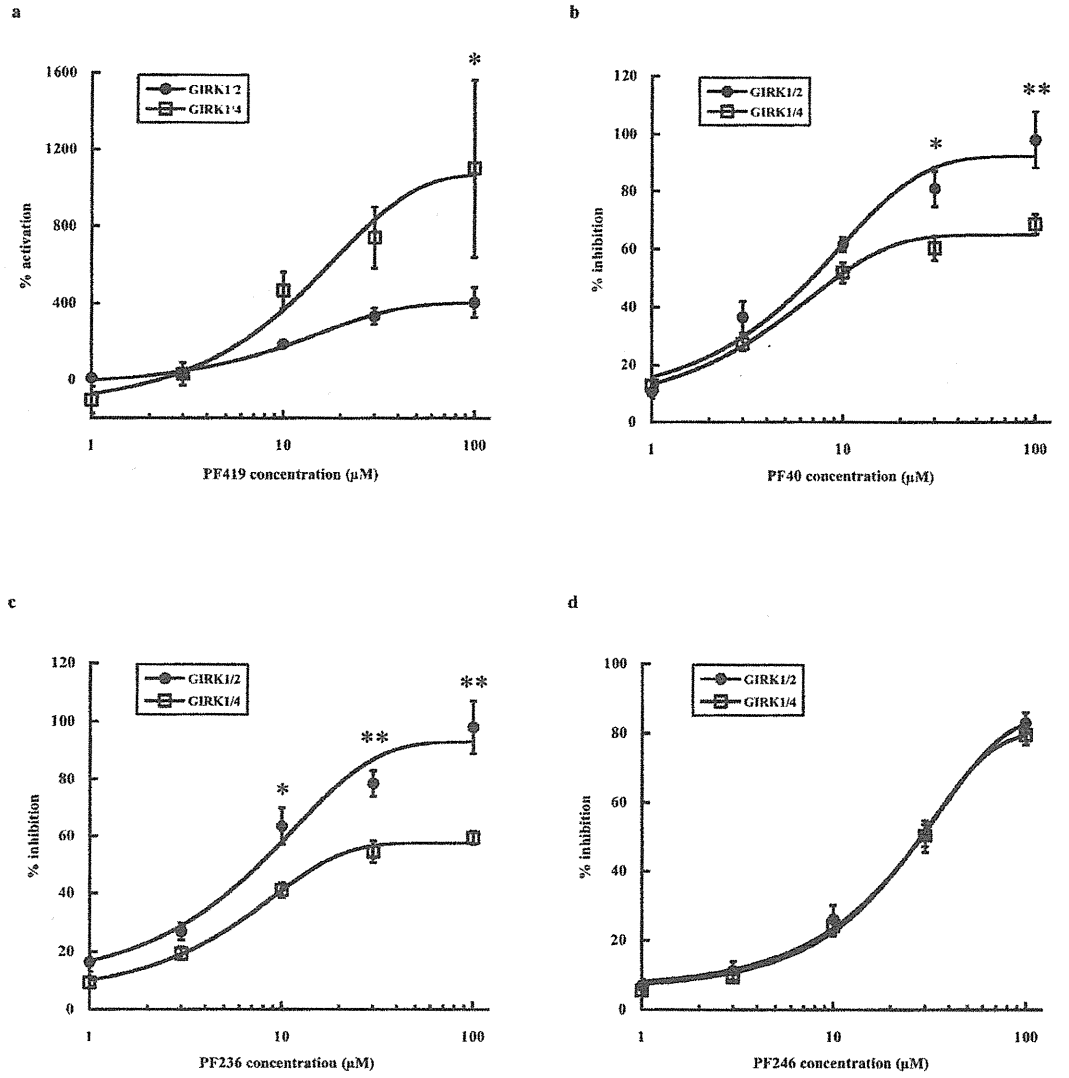


**Fig. (3). Concentration-Response Relationships of the Identified Agonist and Antagonists to GIRK Channels. a.** Current response was normalized by the response to ethanol (100 mM). **b-d.** Current responses were normalized by the response to $BaCl_2$ (2 mM). $*P < 0.005$ between GIRK1/2 and GIRK1/4. $**P < 0.001$ between GIRK1/2 and GIRK1/4.

might be possible that agonists and antagonists were combined in a pool which effectively negated their possible actions on GIRK channels. Therefore, if different combinations of PF compounds had been pooled, different agonists and antagonists might have been identified after the overall screening procedure.

As shown in Table 1, the $IC_{50}$ values for PF 40, PF 236, and PF 246 calculated in the third screening step ranged from 5.98 to 31.2. These were comparable to, or lower than, those of various antipsychotic drugs [14-16], indicating they could be more potent antagonists than therapeutic drugs currently available. In addition, the agonistic effect of PF 419 at 10 μM or higher was several times that of ethanol (100 mM), a well-known GIRK agonist [18, 19], indicating that PF 419 is a very potent GIRK agonist. In a comparison between GIRK1/2 and GIRK1/4, significant differences were observed in PF 419, PF 40, and PF 236 (Fig. 3), suggesting that PF 40 and PF 236 are antagonists relatively selective to GIRK1/2 and PF 419 is an agonist relatively selective to GIRK1/4.

**Table 1. $IC_{50}$ Values of the Antagonists Selected in the Overall Screening**

| | PF40 | PF236 | PF246 |
|---|---|---|---|
| GIRK1/2 | 6.06 | 5.98 | 24 |
| (95%CI) | (4.03-8.68) | (3.09-10.3) | (13.4-55.6) |
| GIRK1/4 | 16.6 | 31.2 | 27.5 |
| (95%CI) | (8.03-44.7) | (15.2-107) | (16.7-54.8) |

CI: confidence intervals.

In conclusion, by screening a total of 503 PF compounds, one compound and three compounds were identified as the most effective agonist and antagonists, respectively. These compounds were all selective for GIRK channels. These effective and GIRK-selective compounds may be useful, therefore, as possible therapeutics for drug dependence and pain.

## ACKNOWLEDGEMENTS

We are grateful to Dr. Toru Kobayashi for his instruction on the experimental techniques and methods of data analyses used in this study. This work was supported by a joint research fund from Pfizer Japan Inc.

## REFERENCES

[1] Jelacic, T.M.; Kennedy, M.E.; Wickman, K.; Clapham, D.E. Functional and biochemical evidence for G-protein-gated inwardly rectifying $K^+$ (GIRK) channels composed of GIRK2 and GIRK3. *J. Biol. Chem.*, **2000**, *275*, 36211-36216.

[2] Kobayashi, T.; Ikeda, K.; Ichikawa, T.; Abe, S.; Togashi, S.; Kumanishi, T. Molecular cloning of a mouse G-protein-activated $K^+$ channel (mGIRK1) and distinct distributions of three GIRK (GIRK1, 2 and 3) mRNAs in mouse brain. *Biochem. Biophys. Res. Commun.*, **1995**, *208*, 1166-1173.

[3] Wickman, K.; Karschin, C.; Karschin, A.; Picciotto, M.R.; Clapham, D.E. Brain localization and behavioral impact of the G-protein-gated $K^+$ channel subunit GIRK4. *J. Neurosci.*, **2000**, *20*, 5608-5615.

[4] Corey, S.; Clapham., D.E. Identification of native atrial G-protein-regulated inwardly rectifying $K^+$ (GIRK4) channel homomultimers. *J. Biol. Chem.*, **1998**, *273*, 27499-27504.

[5] Wickman, K.; Nemec, J.; Gendler, S.J.; Clapham, D.E. Abnormal heart rate regulation in GIRK4 knockout mice. *Neuron*, **1998**, *20*, 103-114.

[6] Ikeda, K.; Kobayashi, T.; Kumanishi, T.; Yano, R.; Sora, I.; Niki, H. Molecular mechanisms of analgesia induced by opioids and ethanol: is the GIRK channel one of the keys? *Neurosci. Res.*, **2002**, *44*, 121-131.

[7] Blednov, Y.A.; Stoffel, M.; Alva, H.; Harris, R.A. A pervasive mechanism for analgesia: activation of GIRK2 channels. *Proc. Natl. Acad. Sci. USA*, **2003**, *100*, 277-282.

[8] Marker, C.L.; Cintora, S.C.; Roman, M.I.; Stoffel, M.; Wickman, K. Hyperalgesia and blunted morphine analgesia in G protein-gated potassium channel subunit knockout mice. *Neuroreport*, **2002**, *13*, 2509-2513.

[9] Marker, C.L.; Lujan, R.; Loh, H.H.; Wickman, K. Spinal G-protein-gated potassium channels contribute in a dose-dependent manner to the analgesic effect of μ- and δ- but not κ-opioids. *J. Neurosci.*, **2005**, *25*, 3551-3559.

[10] Marker, C.L.; Stoffel, M.; Wickman, K. Spinal G-protein-gated $K^+$ channels formed by GIRK1 and GIRK2 subunits modulate thermal nociception and contribute to morphine analgesia. *J. Neurosci.*, **2004**, *24*, 2806-2812.

[11] Mitrovic, I.; Margeta-Mitrovic, M.; Bader, S.; Stoffel, M.; Jan, L.Y.; Basbaum, A.I. Contribution of GIRK2-mediated postsynaptic signaling to opiate and $\alpha_2$-adrenergic analgesia and analgesic sex differences. *Proc. Natl. Acad. Sci. USA*, **2003**, *100*, 271-276.

[12] Morgan, A.D.; Carroll, M.E.; Loth, A.K.; Stoffel, M.; Wickman, K. Decreased cocaine self-administration in Kir3 potassium channel subunit knockout mice. *Neuropsychopharmacology*, **2003**, *28*, 932-938.

[13] Kobayashi, T.; Ikeda, K.; Kumanishi., T. Effects of clozapine on the δ- and κ-opioid receptors and the G-protein-activated $K^+$ (GIRK) channel expressed in *Xenopus* oocytes. *Br. J. Pharmacol.*, **1998**, *123*, 421-426.

[14] Kobayashi, T.; Ikeda, K.; Kumanishi, T. Inhibition by various antipsychotic drugs of the G-protein-activated inwardly rectifying $K^+$ (GIRK) channels expressed in *Xenopus* oocytes. *Br. J. Pharmacol.*, **2000**, *129*, 1716-1722.

[15] Kobayashi, T.; Washiyama, K.; Ikeda, K. Inhibition of G protein-activated inwardly rectifying $K^+$ channels by various antidepressant drugs. *Neuropsychopharmacology*, **2004**, *29*, 1841-1851.

[16] Kobayashi, T.; Washiyama, K.; Ikeda, K. Modulators of G protein-activated inwardly rectifying $K^+$ channels: potentially therapeutic agents for addictive drug users. *Ann. NY Acad. Sci.*, **2004**, *1025*, 590-594.

[17] Kobayashi, T.; Washiyama, K.; Ikeda, K. Inhibition of G protein-activated inwardly rectifying $K^+$ channels by the antidepressant paroxetine. *J. Pharmacol. Sci.*, **2006**, *102*, 278-287.

[18] Kobayashi, T.; Ikeda, K.; Kojima, H.; Niki, H.; Yano, R.; Yoshioka, T.; Kumanishi, T. Ethanol opens G-protein-activated inwardly rectifying $K^+$ channels. *Nat. Neurosci.*, **1999**, *2*, 1091-1097.

[19] Lewohl, J.M.; Wilson, W.R.; Mayfield, R.D.; Brozowski, S.J.; Morrisett, R.A.; Harris, R.A. G-protein-coupled inwardly rectifying potassium channels are targets of alcohol action. *Nat. Neurosci.*, **1999**, *2*, 1084-1090.

[20] Weigl, L.G.; Schreibmayer, W. G protein-gated inwardly rectifying potassium channels are targets for volatile anesthetics. *Mol. Pharmacol.*, **2001**, *60*, 282-289.

[21] keda, K.; Yoshii, M.; Sora, I.; Kobayashi, T. Opioid receptor coupling to GIRK channels. *In vitro* studies using a *Xenopus* oocyte expression system and *in vivo* studies on *weaver* mutant mice. *Methods. Mol. Med.*, **2003**, *84*, 53-64.

[22] Kobayashi, T.; Washiyama, K.; Ikeda, K. Inhibition of G protein-activated inwardly rectifying $K^+$ channels by fluoxetine (Prozac). *Br. J. Pharmacol.*, **2003**, *138*, 1119-1128.

Received: October 01, 2009 Revised: April 17, 2010 Accepted: May 26, 2010

# MOP Reduction During Long-Term Methamphetamine Withdrawal was Restored by Chronic Post-Treatment with Fluoxetine

H. Yamamoto[a,*], Y. Takamatsu[a], K. Imai[b], E. Kamegaya[a], Y. Hagino[a], M. Watanabe[c], T. Yamamoto[a,d], I. Sora[a,e], H. Koga[b] and K. Ikeda[a]

[a]*Division of Psychobiology, Tokyo Institute of Psychiatry, Tokyo, Japan;* [b]*Laboratory for Medical Genomics, Department of Human Genome Technology, Kazusa DNA Research Institute, Chiba, Japan;* [c]*Department of Anatomy, Hokkaido University School of Medicine, Sapporo, Japan;* [d]*Molecular Recognition, Yokohama City University, Yokohama, Japan;* [e]*Department of Psychobiology, Tohoku University, School of Medicine, Sendai, Japan*

**Abstract:** Previously, we found fluoxetine reduces methamphetamine preference in mice. However, effects of fluoxetine on developed methamphetamine preference and on methamphetamine induced gene expression changes have been largely unknown. The present study investigates effects of post-treatment with fluoxetine on methamphetamine dependence and on gene expressions after long-term withdrawal in mice. First, we examined whether chronic post-treatment with fluoxetine attenuated methamphetamine-conditioned place preference. Next, we examined the changes in gene expression levels after long-term withdrawal (with saline or fluoxetine treatment) following chronic methamphetamine treatment. Using mRNA from the pooled frontal cortices of 10 mice per group, gene expression analyses were performed using a custom-developed cDNA array and a real-time quantitative reverse transcription-PCR. Chronic post-treatments with fluoxetine abolished the conditioned place preference developed by methamphetamine administrations. Even after long-term withdrawal from repeated methamphetamine administration, μ-opioid receptor (MOP) gene expression was significantly reduced in the frontal cortex. The reduced MOP gene expression in the frontal cortex was restored by chronic administration with fluoxetine. These changes were confirmed by Western blot analyses. These findings suggest that the chronic post-treatments with fluoxetine might be effective for restoring the reduction of MOP levels in the frontal cortex following long-term abstinence from methamphetamine.

**Keywords:** Methamphetamine, conditioned place preference, gene expression, withdrawal, fluoxetine, mu-opioid receptor, frontal cortex, mice.

## INTRODUCTION

The development process of sensitization to the behavioral effects of psychostimulants is well-researched. There is substantial evidence that the mesocorticolimbic dopamine system and its excitatory glutamatergic inputs are critical [1, 2]. However, glutamate antagonists do not block the expression of sensitization [3]. Similarly, dopamine antagonists can block the development of sensitization to psychostimulants without blocking its expression [4]. On the other hand, glutamatergic afferents from the prefrontal cortex to the ventral tegmental area and the nucleus accumbens have been reportedly implicated in both the development and expression of sensitization to cocaine and amphetamine [5]. The frontal cortex is important region that is activated in addicted subjects during intoxication, craving, and bingeing, and deactivated during withdrawal [6].

Currently, effective pharmacotherapy for psychostimulant abuse has not been established. However, preclinical studies have indicated that the serotonergic system can effectively modulate the behavioral effects of amphetamine. That is, a negative relationship was observed between the potencies of several cocaine- and amphetamine-like drugs in self-administration studies and their binding affinities for serotonin uptake sites [7, 8]. Administration of the serotonin uptake inhibitor fluoxetine decreased self administration of amphetamine [9] in rodents. Amphetamine withdrawal elevates brain reward threshold in rats [10]. Harrison *et al.* (2001) [11] have reported that co-administration of a 5-$HT_{1A}$ receptor antagonist and fluoxetine reverses reward deficits observed during nicotine or amphetamine withdrawal. These findings suggest that increasing brain serotonin activity can attenuate the behavioral and reinforcing effects of amphetamines.

In the present study, we used the frontal cortices of chronically methamphetamine-injected mice to explore molecules that expressions were changed during long-term abstinence and fluoxetine reversed its expressional changes. First, we applied comprehensive approach to exploration of candidate genes by using cDNA array system utilizing mouse KIAA-homologous cDNA (mKIAA) clones. Next, gene expressions and protein expressions were examined by real-time quantitative reverse transcription-polymerase chain reaction (qRT-PCR) experiments and immunoblot analyses, respectively.

*Address correspondence to this author at the Division of Psychobiology, Tokyo Institute of Psychiatry, 2-1-8 Kamikitazawa, Setagaya-ku, Tokyo 156-8585, Japan; Tel: +81-3-3304-5701; Fax: +81-3-3329-8035;
E-mail: yamamoto-hd@igakuken.or.jp

1570-159X/11 $58.00+.00 

## MATERIALS AND METHODS

### Animals

Ten-week-old male C57BL/6J mice were purchased from CLEA Japan (Tokyo, Japan). The experimental procedures and housing conditions were approved by the Tokyo Institute of Psychiatry Institutional Animal Care and Use Committee, and all animals were cared for and treated humanely in accordance with our institutional guidelines on animal experimentation.

### Conditioned Place Preference Test

The conditioned place preference test was performed according to the method of Hoffman and Beninger (1988) [12] with some modifications. For this test, we used a two-compartment Plexiglas chamber (Neuroscience Inc., Osaka, Japan). We selected a counterbalanced protocol to nullify each mouse's initial compartment preference [13].

Acquisition of methamphetamine-induce place preference was shown in drug-naive mice. On Day 1, the mice ($n$ = 18 - 20 per group) were allowed to freely explore the two compartments for 15 min. On Day 2, the same trial was performed, and the time spent in each compartment and shuttle numbers were measured for 15 min. Conditioning was conducted once daily for four consecutive days (Days 5-8). Mice were intraperitoneally (i.p.) injected with methamphetamine (2 mg/kg) and immediately confined to the black or white compartment for 50 min on Day 5. On Day 6, the mice were injected with saline and immediately confined to the opposite compartment for 50 min. On Days 7 and 8, the same conditioning as on Days 5 and 6 was repeated. After methamphetamine conditioning, the mice received saline or fluoxetine (20 mg/kg, i.p.) once a day for 10 days (Days 9–18). On the last day (Day 19), the mice were not treated with saline or fluoxetine. The time spent in each compartment and shuttle numbers were measured for 15 min without methamphetamine injection. Time spent in the drug-paired compartment during pre- and post-conditioning preference tests were analyzed by within-group paired $t$-tests.

### Tissue Preparation, RNA Isolation, Probe Labeling, and Microarray Hybridization

For analysis of gene expression studies, mice in the long-term withdrawal groups were given a saline or methamphetamine injection (2 mg/kg, i.p.) once a day for 14 days, housed for 7 days without any injection, and then injected with saline or fluoxetine (20 mg/kg, i.p.) once a day for 14 days and sacrificed 24 h after the last injection.

After decapitation, the frontal cortices from 10 mice per treatment group were quickly dissected on ice, immediately frozen at -80°C, and used as a pooled sample for the cDNA array experiment [14], qRT-PCR analysis and used as separate samples for western blot analysis.

### qRT-PCR

To confirm the cDNA array results, qRT-PCR was performed on the MOP gene using the TaqMan strategy (Mm01188089 m1) and the ABI Prism 7300 Sequence Detection System (Applied Biosystems, Foster City, CA). For the expression of the genes other than the MOP gene, real-time qRT-PCR was performed using a cybergreen fluorescence-based assay kit (SBYR Green RT-PCR kit; Takara Bio Inc., Shiga, Japan) according to the manufacturer's instructions. The levels of all cDNAs generated from mRNA by reverse transcription were calculated by the standard curve method for quantification and normalized with respect to GAPDH transcript levels.

### Western Blotting

$P_2$ membranes were prepared from homogenate derived from each frontal cortex. Samples were mixed with an equal volume of Laemmli's samples buffer (10 μg/lane), boiled for 3 min and then resolved on a 5-20% gradient SDS polyacrylamide gel electrophoresis. The proteins were electrotransferred onto PVDF membranes in a semi-dry blotter.

We used two rabbit polyclonal antibodies specific for MOP. *N*-terminal-specific antiserum (N-38) was prepared against 1–38 amino acids sequences of the MOP *N*-terminus [15]. The *C*-terminus-specific antibody (AB5511, lot No. 25050663) was purchased from Chemicon International (Temecula, CA, USA). Rabbit polyclonal anti-actin antibody was purchased from Sigma-Aldrich (St. Louis, MO, USA) and used to detect endogenous actin as an internal standard.

### Statistical Analysis

Parametric analysis of quantitative data was performed using a one-way analysis of variance (ANOVA) followed by Scheffe's test. Nonparametric analysis was conducted using the Kruskal-Wallis test followed by Scheffe's *post hoc* comparison test. The level of statistical significance was set at $p < 0.05$.

## RESULTS

### Effects of Chronic Administration of Fluoxetine on Methamphetamine-Induced Conditioned Place Preference

Time spent in the conditioned compartment was significantly increased when saline was administered for 9 days after methamphetamine conditioning ($n$ = 20, $t$ = 4.408, $p$ = 0.0003; Fig. (**1A**)). By contrast, time spent in the conditioned compartment was not significantly changed when fluoxetine (20 mg/kg) was administered for 9 days after methamphetamine conditioning ($n$ = 18, $t$ = 1.513, $p$ = 0.1488; Fig. (**1B**)). These results suggest that subchronic administration of fluoxetine at a dose of 20 mg/kg to mice weakened the place preference induced by methamphetamine. Thus next, we used mice chronically treated with fluoxetine (20 mg/kg) during methamphetamine withdrawal in the gene expression and western blot analyses.

### Effects of Fluoxetine on Methamphetamine-Induced Changes in Gene Expression after Long-Term Withdrawal

In the cDNA array experiments, expressions of a few genes, MOP, N-methyl-D-aspartate (NMDA) receptor 2D subunit (NR2D), nociceptin receptor, G protein-activated inwardly rectifying $K^+$ channels (GIRKs) and inward rectifier $K^+$ channel Kir2.3 (IRK3), were reduced after 3 weeks withdrawal following chronic methamphetamine treatment (MAP-Saline column in Table **1**). These reductions (< 70 %

reduction in the saline treatment) were recovered in some genes except GIRK1 and GIRK3 when treated with fluoxetine for 2 weeks after the chronic methamphetamine treatment (MAP-Flx in Table 1). The cDNA array experiments were performed in multiple determinations using a set of pooled samples.

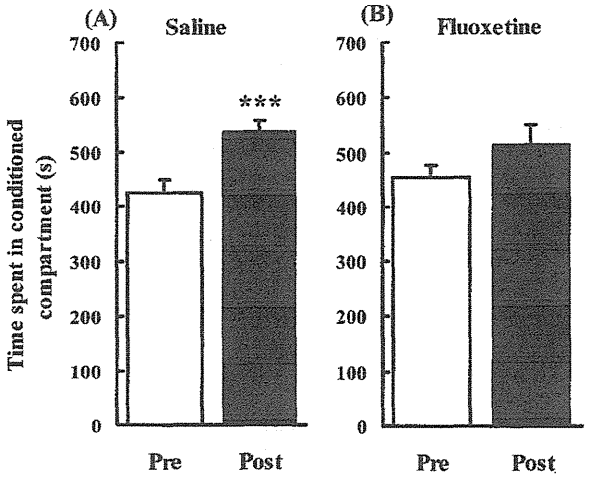


**Fig. (1).** Effects of chronic administration of fluoxetine on the established methamphetamine-induced conditioned place preference. After methamphetamine conditioning, mice received (**A**) saline or (**B**) fluoxetine for 9 days. Each bar represents mean ± SEM of the time spent in the methamphetamine-paired compartment during a 15-min test session. Pre: preference test during the pre-conditioning phase. Post: preference test during the post-conditioning phase. ***: difference between Pre and Post, $p < 0.001$.

To assess data derived from cDNA array, we performed qRT-PCR analyses on these gene expressions using mRNA derived from three sets of pooled cortices. The qRT-PCR data were shown in parenthesis in Table 1. Expressions of mu-opioid receptor and IRK3 were approximately similar between cDNA array and qRT-PCR analyses. However, gene expressions of NR2D, nociceptin receptor and GIRK2 were not reduced after 3 weeks withdrawal following chronic methamphetamine treatment (parenthesis of MAP-Saline column in Table 1). On the other hand, reduced expression (MAP-Saline) of mu-opioid receptor was recovered by fluoxetine treatment til 93%, while that of IRK3 was 35% (parenthesis of % recovery by fluoxetine treatment in Table 1).

Results using cDNA array experiment and qRT-PCR analyses had shown that the reduced gene expression of MOP in the frontal cortex during long-term withdrawal was restored by subsequent fluoxetine treatments.

### Fluoxetine Effects on MOP-Immunoreactivity

To investigate the results obtained from the gene expression analyses, immunoblot of MOP in each frontal cortex of methamphetamine-injected mouse was performed (4 – 12 mice per group). MOP-immunoreactivity (IR) in the frontal cortex was detected as a broad band at a position consistent with a molecular weight of 65,000 with anti-MOP sera (N-38 and AB5511) (Fig. (**2A**)). These two anti-MOP sera (N-38 and AB5511) were specific against MOP molecule. The detected broad bands by these antisera were abolished using MOP knockout mice. MOP-IR with AB5511 antibody of the MAP-Saline sample (3-week withdrawal with saline injections after chronic methamphetamine injections, $n = 11$) was significantly lower than that of the Saline-Saline sample (3-week withdrawal with saline injections after chronic saline injections, $n = 12$) ($p = 0.0101$; Fig. (**2B**)). The intensity of MOP-IR in the MAP-Flx sample (3-week withdrawal with fluoxetine injections after chronic methamphetamine injections, $n = 4$) was significantly higher than that in the MAP-Saline sample ($p = 0.0203$; Fig. (**2B**)) and not different from that in the Saline-Saline sample ($p = 0.902$). The intensity of MOP-IR in the Saline-Flx sample (3-week withdrawal with fluoxetine injections after chronic saline injections, $n = 6$) was not significantly different from those in the Saline-Saline and MAP-Flx samples ($p = 0.699$; $p = 0.473$). These results have shown that MOP-IR was reduced after 3 weeks withdrawal following chronic methamphetamine treatment and this reduction was recovered by subsequent fluoxetine treatments.

## DISCUSSION

In the present study, repeated methamphetamine administration induced a conditioned place preference. The place preference was significantly attenuated by chronic fluoxetine treatments during long-term withdrawal. Fluoxetine is reported to reverse reward deficits during amphetamine withdrawal [11]. Recently, Kaneko *et al.* (2007) [16] reported that 5-day treatment with fluoxetine and paroxetine during methamphetamine withdrawal may at least in part reverse methamphetamine-induced behavioral sensitization. Taken together, these results suggest that chronic fluoxetine treatment can partially reverse methamphetamine-induced behavioral changes.

We observed that 3-week withdrawal after chronic methamphetamine induced gene expression changes. Of interest, both in the cDNA array and the real-time qRT-PCR analyses, MOP gene expression was decreased in the frontal cortex after long-term withdrawal, and partially restored by chronic fluoxetine treatment during methamphetamine withdrawal. On the basis of these results of gene expressions, we have performed the protein expressions of MOP by western blot analysis. Of interest, immunoreactive MOP level was significantly reduced during methamphetamine withdrawal, while chronic fluoxetine administrations during withdrawal could partially restore the reduced MOP expression level in the frontal cortex.

To date, changes in MOP expression after withdrawal from alcohol and amphetamine have been reported. Lower MOP binding potential in the right dorsal lateral prefrontal cortex, the right anterior frontal cortex, and the right parietal cortex is associated with higher craving in male alcohol-dependent subjects undergoing alcohol withdrawal [17], even though after long-term abstinence alcoholic patients display no changes in the prefrontal cortex but an increase in the binding potential of MOP in the ventral striatum, including the nucleus accumbens [18]. In contrast, subchronic injections of amphetamine resulted in a significant reduction in MOP mRNA levels in the nucleus accumbens shell [19], whereas no significant changes were observed in the level of

**Table 1. Effect of Chronic Fluoxetine Treatment on Changes in Gene Expression After Long-Term Withdrawal Following Chronic Methamphetamine Injections**

| cDNA Array Result (RT-PCR Result) | | | | | | |
|---|---|---|---|---|---|---|
| Entrez | | Gene(Property) | MAP-Saline | MAP-Flx | Saline-Flx | % of Recovery |
| Official Symbol | Gene ID | | | (% of Saline-Saline Control) | | by Flx Treatment |
| **Receptors** | | | | | | |
| Htr2c | 15560 | 5HTR1C | 88.5 | 78.3 | 88.9 | |
| Htr1e | 107927 | 5HTR1E | 94.8 | 85.5 | 107.6 | |
| Htr2a | 15558 | 5HTR2A | 108.3 | 102.6 | 113.1 | |
| Adra2a | 11551 | alpha2AR | 115.5 | 93.8 | 97.5 | |
| Bzrap1 | 207777 | benzodiazapine receptor (peripheral) associated protein 1 | 88.0 | 90.0 | 82.4 | |
| Oprd1 | 18386 | delta-opioid receptor | 74.2 | 90.0 | 90.0 | |
| Esrrg | 26381 | estrogen-related receptor gamma | 80.4 | 74.6 | 83.4 | |
| Oprk1 | 18387 | kappa-opioid receptor | 80.4 | 101.8 | 115.1 | |
| Lepr | 16847 | leptin R | 95.8 | 90.7 | 99.3 | |
| Sigmar1 | 18391 | Sigma-1 receptor | 87.9 | 83.4 | 96.5 | |
| Oprm1 | 18390 | mu-opioid receptor | 58.5 (75.0) | 83.4 (98.2) | 86.4 (90.1) | 60.0 (92.8) |
| Grm1 | 14816 | mGluR1 | 105.0 | 117.5 | 120.5 | |
| Grm5 | 108071 | mGluR5 | 84.3 | 82.6 | 98.7 | |
| Npy2r | 18167 | neuropeptideY-Y2 receptor | 93.4 | 93.2 | 84.5 | |
| Grin2b | 14812 | NR2B | 70.1 | 78.0 | 96.1 | |
| Grin2c | 14813 | NR2C | 85.9 | 79.7 | 92.3 | |
| Grin2d | 14814 | NR2D | 60.8 (95.3) | 64.5 (80.7) | 84.2 (88.2) | 9.4 |
| Grin1 | 14810 | NR1 | 88.9 | 104.8 | 95.7 | |
| Oprl1 | 18389 | nociceptin receptor | 68.8 (102) | 91.1 (92.2) | 81.5 (92.4) | 71.6 |
| Ogfr | 72075 | opioid growth factor receptor | 94.2 | 105.9 | 112.7 | |
| **Ion Channels** | | | | | | |
| Cacna2d2 | 56808 | calcium channel, voltage-dependent, | 86.4 | 103.2 | 90.8 | |
| Kcnj3 | 16519 | GIRK1 | 63.4 | 54.4 | 70.9 | |
| Kcnj6 | 16522 | GIRK2 | 66.1 (92.5) | 79.0 (106) | 78.7 (98.3) | 38.2 |
| Kcnj9 | 16524 | GIRK3 | 57.5 | 54.4 | 71.9 | |
| Kcnj12 | 16515 | IRK2 | 72.3 | 102.0 | 96.1 | |
| Kcnj4 | 16520 | IRK3 | 63.7 (67.3) | 76.4 (78.8) | 93.1 (70.8) | 34.8 |
| Kcns2 | 16539 | $K^+$ voltage-gated channel, subfamily S, 2 | 112.3 | 123.9 | 122.9 | |
| Rims3 | 242662 | $K^+$ channel, subfamily K, member 15 and regulating synaptic membrane exocytosis 3 | 95.0 | 95.9 | 123.6 | |
| Kcnt1 | 227632 | $K^+$ channel, subfamily T, member 1 | 83.1 | 95.8 | 80.2 | |
| Kcnd2 | 16508 | $K^+$ voltage-gated channel, Shal-related subfamily | 76.3 | 83.5 | 97.2 | |
| Scn3b | 235281 | $Na^+$ channel, voltage-gated, type III, beta | 90.5 | 94.5 | 99.3 | |

The qRT-PCR data were shown in parenthesis in Table 1.

Treatment for 2 weeks with saline followed by two weeks with saline (Saline-Saline); treatment for 2 weeks with methamphetamine followed by 2 weeks with saline (MAP-Saline); treatment for 2 weeks with methamphetamine followed by 2 weeks with fluoxetine (MAP-Flx); and treatment for 2 weeks with saline followed by 2 weeks with fluoxetine (Saline-Flx).

Data are presented as percentages of Saline-Saline group, representing the mean ± SEM of 4-16 determinations of pooled samples.

Percentage of recovery was calculated as follows: (1-{(100-[MAP-Flx]value) / (100-[MAP-Saline]value)}) x 100.

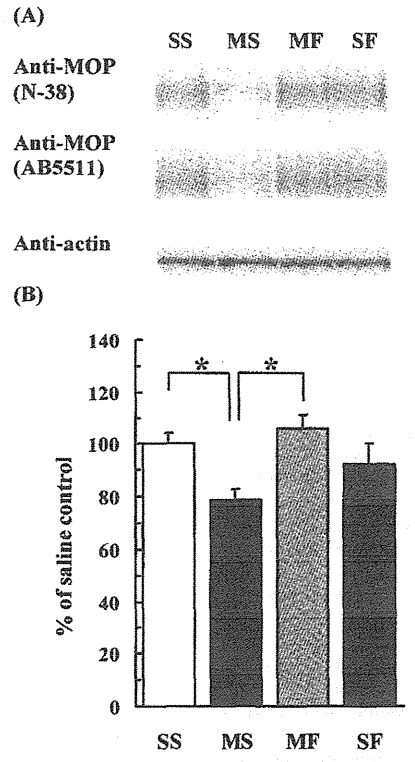


**Fig. (2).** Immunoblot analyses of changes in MOP protein levels in the frontal cortex by saline or methamphetamine treatment followed by saline or fluoxetine treatment. (**A**) Typical immunoblot with anti-MOP and anti-actin antibodies. Using antiserum selective for MOP *N*-terminal (N-38) or *C*-terminal (AB5511), similar broad bands were detected using the same membrane. Actin levels were measured as references. (**B**) Quantitation of densitometer values using antiserum (AB5511). Values were normalized using actin values and represented as percentage of saline control values. Each bar represents the mean ± SEM of more than four individual mouse frontal cortices. Treatment for 2 weeks with saline followed by two weeks with saline (saline-saline [SS] sample, $n = 12$); treatment for 2 weeks with methamphetamine followed by 2 weeks with saline (methamphetamine-saline [MS] sample, $n = 11$); treatment for 2 weeks with methamphetamine followed by 2 weeks with fluoxetine (methamphetamine-fluoxetine [MF] sample, $n = 4$); and treatment for 2 weeks with saline followed by 2 weeks with fluoxetine (saline-fluoxetine [SF] sample, $n = 6$). *: difference between methamphetamine-saline group and saline-saline group or methamphetamine-fluoxetine group, $p < 0.05$, ANOVA.

MOP mRNA expressed in the nucleus accumbens shell of behaviorally sensitized rats tested 2 or 14 days after withdrawal [20]. Recently, Chiu *et al.* (2006) [21] have used the whole brain except cerebellum repeatedly injected with 2.5 mg/kg of methamphetamine for 7 days and reported that maximal binding of MOP is not changed on days 2 and 5, but down-regulated on day 8. After cessation of drug treatments, the maximal binding of MOP returns to normal level on day 11 and up-regulates on day 21. These data are of interest considering that the expressions of behavioral sensitization were attenuated by pretreatment with 10 or 20 mg/kg of naltrexone either during the induction period or before methamphetamine challenge when they were tested on days 11 and 21 [22]. However they also mention that whole brain samples may be insufficient to reveal the region-specific changes [21]. Investigating methamphetamine-induced craving, endogenous opioid system is involved in the mechanisms underlying cue-induced relapse [23]. Naltrexone inhibits reinstatement of drug-seeking behavior induced by methamphetamine-associated cues, but has no effect on methamphetamine-priming-induced reinstatement. The implication of these results is that there are distinct mechanisms underlying drug-seeking behavior induced by re-exposure to drug-associated cues and that induced by drug priming. Further, the results indicate that increasing activity of the opioid system is involved in the cue-induced drug-seeking behavior, but not in that induced by drug-priming [23]. Naltrexone pretreatment also attenuates context-induced alcohol seeking and inhibits c-fos mRNA expression in the basolateral amygdala and the CA3 subregion of the hippocampus [24]. Therefore, regional specificity is important to study methamphetamine induced behaviors, including conditioned place preference, drug-seeking behavior and behavioral sensitization. To our knowledge, this is the first report of reduced MOP expression in the frontal cortex of long-term methamphetamine withdrawal detected by gene expression and protein expression analyses. This result would provide important insight into the relationship between mu-opioid receptor in the frontal cortex and methamphetamine induced behaviors.

In humans, Ide *et al.* (2006) [25] have shown associations between MOP gene (*OPRM1*) polymorphisms and methamphetamine dependence/psychosis. They also found significant differences in both genotype and allele frequencies of single-nucleotide polymorphisms (SNPs) in the *OPRM1* gene between control and methamphetamine-dependent/psychotic patients. There also is a significant association between SNPs and patients with transient psychosis. These findings suggest that MOP function may affect the development of methamphetamine psychosis. MOP also may be a key molecule involved in the mechanisms underlying behavioral changes after long-term withdrawal following chronic methamphetamine treatment.

In conclusion, the present study showed that reduced mRNA and protein expressions of MOP gene were found in the frontal cortex of methamphetamine-abuse model mice even after long-term abstinence. Furthermore, the subchronic fluoxetine treatment during methamphetamine withdrawal restored MOP expressions. Although the mechanisms underlying the therapeutic effect of fluoxetine for methamphetamine abuse should be further investigated, we suggest a possibility that the restoration of MOP expression can be used as one of therapeutic markers for drug dependence.

## ACKNOWLEDGEMENTS

This work was supported by grants from the MEXT (17025054), MHLW (H19-Iyaku-023, H17-Pharmaco-001, H16-Iyaku-029, 18A-3 for Nervous and Mental Disorders), The Naito Foundation, and Foundation for Promotion of Material Science and Technology of Japan (MST). We are grateful to Dr. Makoto Honda for his helpful instruction regarding qRT-PCR analysis and to Dr. Yasukazu Ogai for his excellent advice on statistical analysis.

## REFERENCES


[1] Carlezon, W.A., Jr.; Nestler, E.J. Elevated levels of GluR1 in the midbrain: a trigger for sensitization to drugs of abuse? *Trends Neurosci.*, **2002**, *25*, 610-615.

[2] Wolf, M.E.; Sun, X.; Mangiavacchi, S.; Chao, S.Z. Psychomotor stimulants and neuronal plasticity. *Neuropharmacology*, **2004**, *47* (Suppl 1), 61-79.

[3] Wolf, M.E.; Jeziorski, M. Coadministration of MK-801 with amphetamine, cocaine or morphine prevents rather than transiently masks the development of behavioral sensitization. *Brain Res.*, **1993**, *613*, 291-294.

[4] Weiss, S.R.; Post, R.M.; Pert, A.; Woodward, R.; Murman, D. Context-dependent cocaine sensitization: differential effect of haloperidol on development versus expression. *Pharmacol. Biochem. Behav.*, **1989**, *34*, 655-661.

[5] Wolf, M.E.; Dahlin, S.L.; Hu, X.T.; Xue, C.J.; White, K. Effects of lesions of prefrontal cortex, amygdala, or fornix on behavioral sensitization to amphetamine: comparison with N-methyl-D-aspartate antagonists. *Neuroscience*, **1995**, *69*, 417-439.

[6] Goldstein, R.Z.; Volkow, N.D. Drug addiction and its underlying neurobiological basis: neuroimaging evidence for the involvement of the frontal cortex. *Am. J. Psychiatry*, **2002**, *159*, 1642-1652.

[7] Ritz, M.C.; Kuhar, M.J. Relationship between self-administration of amphetamine and monoamine receptors in brain: comparison with cocaine. *J. Pharmacol. Exp. Ther.*, **1989**, *248*, 1010-1017.

[8] Ritz, M.C.; Lamb, R.J.; Goldberg, S.R.; Kuhar, M.J. Cocaine receptors on dopamine transporters are related to self-administration of cocaine. *Science*, **1987**, *237*, 1219-1223.

[9] Porrino, L.J.; Ritz, M.C.; Goodman, N.L.; Sharpe, L.G.; Kuhar, M.J.; Goldberg, S.R. Differential effects of the pharmacological manipulation of serotonin systems on cocaine and amphetamine self-administration in rats. *Life Sci.*, **1989**, *45*, 1529-1535.

[10] Cryan, J.F.; Hoyer, D.; Markou, A. Withdrawal from chronic amphetamine induces depressive-like behavioral effects in rodents. *Biol. Psychiatry*, **2003**, *54*, 49-58.

[11] Harrison, A.A.; Liem, Y.T.; Markou, A. Fluoxetine combined with a serotonin-1A receptor antagonist reversed reward deficits observed during nicotine and amphetamine withdrawal in rats. *Neuropsychopharmacology*, **2001**, *25*, 55-71.

[12] Hoffman, D.C.; Beninger, R.J. Selective D1 and D2 dopamine agonists produce opposing effects in place conditioning but not in conditioned taste aversion learning. *Pharmacol. Biochem. Behav.*, **1988**, *31*, 1-8.

[13] Ide, S.; Minami, M.; Satoh, M.; Uhl, G.R.; Sora, I.; Ikeda, K. Buprenorphine antinociception is abolished, but naloxone-sensitive reward is retained, in mu-opioid receptor knockout mice. *Neuropsychopharmacology*, **2004**, *29*, 1656-1663.

[14] Yamamoto, H.; Imai, K.; Takamatsu, Y.; Kamegaya, E.; Kishida, M.; Hagino, Y.; Hara, Y.; Shimada, K.; Yamamoto, T.; Sora, I.; Koga, H.; Ikeda, K. Methamphetamine modulation of gene expression in the brain: analysis using customized cDNA microarray system with the mouse homologues of KIAA genes. *Brain Res. Mol. Brain Res.*, **2005**, *137*, 40-46.

[15] Kasai, S.; Yamamoto, H.; Kamegaya, E.; Uhl, G.R.; Sora, I.; Watanabe, M.; Ikeda, K. Mu-opioid peptide receptors (MOPS) are detected as broad bands around 65 kDa in western blotting: analyses using MOP knockout mice. *Curr. Neuropharmacol.*, ***in press***.

[16] Kaneko, Y.; Kashiwa, A.; Ito, T.; Ishii, S.; Umino, A.; Nishikawa, T. Selective serotonin reuptake inhibitors, fluoxetine and paroxetine, attenuate the expression of the established behavioral sensitization induced by methamphetamine. *Neuropsychopharmacology*, **2007**, *32*, 658-664.

[17] Bencherif, B.; Wand, G.S.; McCaul, M.E.; Kim, Y.K.; Ilgin, N.; Dannals, R.F.; Frost, J.J. Mu-opioid receptor binding measured by [$^{11}$C]carfentanil positron emission tomography is related to craving and mood in alcohol dependence. *Biol. Psychiatry*, **2004**, *55*, 255-262.

[18] Heinz, A.; Reimold, M.; Wrase, J.; Hermann, D.; Croissant, B.; Mundle, G.; Dohmen, B.M.; Braus, D.F.; Schumann, G.; Machulla, H.J.; Bares, R.; Mann, K. Correlation of stable elevations in striatal mu-opioid receptor availability in detoxified alcoholic patients with alcohol craving: a positron emission tomography study using carbon 11-labeled carfentanil. *Arch. Gen. Psychiatry*, **2005**, *62*, 57-64.

[19] Vecchiola, A.; Collyer, P.; Figueroa, R.; Labarca, R.; Bustos, G.; Magendzo, K. Differential regulation of mu-opioid receptor mRNA in the nucleus accumbens shell and core accompanying amphetamine behavioral sensitization. *Brain Res. Mol. Brain Res.*, **1999**, *69*, 1-9.

[20] Magendzo, K.; Bustos, G. Expression of amphetamine-induced behavioral sensitization after short- and long-term withdrawal periods: participation of mu- and delta-opioid receptors. *Neuropsychopharmacology*, **2003**, *28*, 468-477.

[21] Chiu, C.T.; Ma, T.; Ho, I.K. Methamphetamine-induced behavioral sensitization in mice: alterations in mu-opioid receptor. *J. Biomed. Sci.*, **2006**, *13*, 797-811.

[22] Chiu, C.T.; Ma, T.; Ho, I.K. Attenuation of methamphetamine-induced behavioral sensitization in mice by systemic administration of naltrexone. *Brain Res. Bull.*, **2005**, *67*, 100-109.

[23] Anggadiredja, K.; Sakimura, K.; Hiranita, T.; Yamamoto, T. Naltrexone attenuates cue- but not drug-induced methamphetamine seeking: a possible mechanism for the dissociation of primary and secondary reward. *Brain Res.*, **2004**, *1021*, 272-276.

[24] Marinelli, P.W.; Funk, D.; Juzytsch, W.; Li, Z.; Le, A.D. Effects of opioid receptor blockade on the renewal of alcohol seeking induced by context: relationship to c-fos mRNA expression. *Eur. J. Neurosci.*, **2007**, *26*, 2815-2823.

[25] Ide, S.; Kobayashi, H.; Ujike, H.; Ozaki, N.; Sekine, Y.; Inada, T.; Harano, M.; Komiyama, T.; Yamada, M.; Iyo, M.; Iwata, N.; Tanaka, K.; Shen, H.; Iwahashi, K.; Itokawa, M.; Minami, M.; Satoh, M.; Ikeda, K.; Sora, I. Linkage disequilibrium and association with methamphetamine dependence/psychosis of mu-opioid receptor gene polymorphisms. *Pharmacogenomics J.*, **2006**, *6*, 179-188.


Received: October 01, 2009 Revised: April 17, 2010 Accepted: May 26, 2010

Psychiatry Research 187 (2011) 312–313

Contents lists available at ScienceDirect

Psychiatry Research

journal homepage: www.elsevier.com/locate/psychres

Letter to the editor

## Association study on catechol-O-methyltransferase (*COMT*) Val158Met gene polymorphism and NEO-FFI

The *COMT* Val158Met gene polymorphism (rs4680) is associated with psychiatric diseases; the Val allele is associated with higher enzymatic activity than the Met allele (Lotta et al., 1995; Lachman et al., 1996), and it may be related to personality traits.

Association studies on the Val158Met polymorphism and personality traits have been reported, but their results are inconsistent (Eley et al., 2003; Stein et al., 2005; Tochigi et al., 2006; Urata et al., 2007).

We attempted to identify the genetic factors affecting personality traits by examining the association between the Val158Met polymorphism and personality traits, using the Neuroticism Extraversion Openness-Five Factor Inventory (NEO-FFI).

This study was approved by the ethics committee of Azabu University. Blood samples were collected from 143 healthy Japanese adults (40 men and 103 women; mean age, $19.9 \pm 1.06$ years) after obtaining their written informed consent. They were then evaluated using the NEO-FFI. Genotyping was performed using polymerase chain reaction–restriction fragment length polymorphism (PCR-RFLP) (Erdal et al., 2001). We compared the NEO-FFI scores among the genotypes by performing statistical analysis using one-way analysis of covariance (ANCOVA) with age as a covariate, and Bonferroni's multiple comparisons for adjusted mean values were used as *post-hoc* tests. We applied a Bonferroni correction of a factor of 3 because the three multiple tests are the association of Val/Val, Val/Met, and Met/Met with NEO-FFI scores.

The genotype distribution for the entire participant population was in the Hardy–Weinberg equilibrium ($\chi^2$ (1) = 0.056, $P = 0.813$, with Yates' continuity correction). In all the subjects, agreeableness, as measured by the NEO-FFI, was significantly associated with genotypes ($F$ (2, 139) = 3.44; $P = 0.035$). Multiple comparisons showed that the Val/Val genotype had significantly lower scores than the Val/Met genotype ($P = 0.044$); significant differences in agreeableness and consciousness were observed between individuals with and without the Met allele ($F(1, 140) = 6.92$, $P = 0.010$; $F(1, 140) = 4.54$, $P = 0.035$). Separate analysis of each sex showed that agreeableness was associated with genotypes only in males ($F$ (1, 36) = 4.61, $P = 0.016$). Multiple comparisons showed that the Val/Val genotype exhibited lower scores than the Val/Met genotype ($P = 0.014$); a significant difference in agreeableness in males was observed between the individuals with and without the Met allele ($F$ (1, 37) = 9.34, $P = 0.004$). Moreover, conscientiousness was associated with genotypes only in females ($F$ (2, 99) = 3.89, $P = 0.024$); however, multiple comparisons showed no significant differences. Meanwhile, a significant difference in conscientiousness in females was observed between the individuals with and without the Met allele ($F(1, 100) = 7.14$, $P = 0.009$).

We found that the Val158Met polymorphism may be associated with personality traits.

The NEO-FFI scales showed a significant relationship between this polymorphism and TCI were different in males and females; therefore, physiological reactivity induced by a change in dopamine concentration may be different for each sex. Our results suggest that this polymorphism is associated with agreeableness and conscientiousness, and as far as we know, similar results have not yet been reported. Only single gene polymorphisms are significantly associated with personality traits; therefore, this polymorphism may be an important factor affecting personality traits.

Furthermore, association studies between the Val158Met polymorphism and prefrontal cortex (PFC) function have been performed using the Wisconsin card sorting test (WCST) and the n-back task (Egan et al., 2001; Malhotra et al., 2002; Goldberg et al., 2003; Caldu et al., 2007). Egan et al. reported that fewer perseverative errors occurred in the following order: Met/Met>Val/Met>Val/Val (Egan et al., 2001). The change in the PFC function may affect personality traits.

Further detailed studies may be required to examine the gene polymorphisms of other enzymes involved in the metabolic pathway of the dopamine system.

### Acknowledgements

This research was partially supported by The Promotion and Mutual Aid Corporation for Private Schools of Japan, Grant-in-Aid for Matching Fund Subsidy for Private Universities.

### References

Caldu, X., Vendrell, P., Bartres-Faz, D., Clemente, I., Bargallo, N., Jurado, M.A., Serra-Grabulosa, J.M., Junque, C., 2007. Impact of the COMT Val108/158Met and DAT genotypes on prefrontal function in healthy subjects. Neuroimage 37, 1437–1444.

Egan, M.F., Goldberg, T.E., Kolachana, B.S., Callicott, J.H., Mazzanti, C.M., Straub, R.E., Goldman, D., Weinberger, D.R., 2001. Effect of COMT Val108/158Met genotype on frontal lobe function and risk for schizophrenia. Proceedings of the National Academy of Sciences of the United States of America 98, 6917–6922.

Eley, T.C., Tahir, E., Angleitner, A., Harriss, K., McClay, J., Plomin, R., Riemann, R., Spinath, F., Craig, I., 2003. Association analysis of MAOA and COMT with neuroticism assessed by peers. American Journal of Medical Genetics 120B, 90–96.

Erdal, M.E., Herken, H., Yilmaz, M., Bayazit, Y.A., 2001. Significance of the catechol-O-methyltransferase gene polymorphism in migraine. Brain Research. Molecular Brain Research 94, 193–196.

Goldberg, T.E., Egan, M.F., Gscheidle, T., Coppola, R., Weickert, T., Kolachana, B.S., Goldman, D., Weinberger, D.R., 2003. Executive subprocesses in working memory: relationship to catechol-O-methyltransferase Val158Met genotype and schizophrenia. Archives of General Psychiatry 60, 889–896.

Lachman, H.M., Papolos, D.F., Saito, T., Yu, Y.M., Szumlanski, C.L., Weinshilboum, R.M., 1996. Human catechol-O-methyltransferase pharmocogenetics: description of a functional polymorphism and its potential application to neuropsychiatric disorders. Pharmacogenetics 6, 243–250.

Lotta, T., Vidgren, J., Tilgmann, C., Ulmanen, I., Melen, K., Julkunen, I., Taskinen, J., 1995. Kinetics of human soluble and membrane-bound catechol O-methyltransferase: a revised mechanism and description of the thermolabile variant of the enzyme. Biochemistry 34, 4202–4210.

Malhotra, A.K., Kestler, L.J., Mazzanti, C., Bates, J.A., Goldberg, T., Goldman, D., 2002. A functional polymorphism in the COMT gene and performance on a test of prefrontal cognition. The American Journal of Psychiatry 159, 652–654.

Stein, M.B., Fallin, M.D., Schork, N.J., Gelernter, J., 2005. COMT polymorphisms and anxiety-related personality traits. Neuropsychopharmacology 30, 2092–2102.

Tochigi, M., Otowa, T., Hibino, H., Kato, C., Otani, T., Umekage, T., Utsumi, T., Kato, N., Sasaki, T., 2006. Combined analysis of association between personality traits and three functional polymorphisms in the tyrosine hydroxylase, monoamine oxidase A, and catechol-O-methyltransferase genes. Neuroscience Research 54, 180–185.

0165-1781/$ - see front matter 
doi:10.1016/j.psychres.2010.09.015

Urata, T., Takahashi, N., Hakamata, Y., Iijima, Y., Kuwahara, N., Ozaki, N., Ono, Y., Amano, M., Inada, T., 2007. Gene-gene interaction analysis of personality traits in a Japanese population using an electrochemical DNA array chip analysis. Neuroscience Letters 414, 209–212.

Jun Aoki
*Laboratory of Neurophysiology, The Graduate School of Environmental Health Sciences, Azabu University, 1-17-71 Fuchinobe, Sagamihara-shi, Kanagawa 229-8501, Japan*
*Division of Psychobiology, Tokyo Institute of Psychiatry, Setagaya-ku, Tokyo 156-8585, Japan*
*Department of Neuropsychiatry, Tokyo Women's Medical University, Shinjuku-ku, Tokyo 162-8666, Japan*

Kazuhiko Iwahashi
*Laboratory of Neurophysiology, The Graduate School of Environmental Health Sciences, Azabu University, 1-17-71 Fuchinobe, Sagamihara-shi, Kanagawa 229-8501, Japan*
*Division of Psychobiology, Tokyo Institute of Psychiatry, Setagaya-ku, Tokyo 156-8585, Japan*
*Department of Neuropsychiatry, Tokyo Women's Medical University, Shinjuku-ku, Tokyo 162-8666, Japan*
*Health Administration Center, Azabu University, 1-17-71 Fuchinobe, Sagamihara-shi, Kanagawa 229-8501, Japan*
Corresponding author. Health Administration Center, Azabu University, 1-17-71 Fuchinobe, Sagamihara-shi, Kanagawa 229-8501, Japan.
Tel./fax: +81 42 769 1930.
*E-mail address:* iwahashi@azabu-u.ac.jp.

Jun Ishigooka
*Department of Neuropsychiatry, Tokyo Women's Medical University, Shinjuku-ku, Tokyo 162-8666, Japan*

Kazutaka Ikeda
*Division of Psychobiology, Tokyo Institute of Psychiatry, Setagaya-ku, Tokyo 156-8585, Japan*

20 March 2009

Ide et al. Molecular Pain 2011, 7:23
http://www.molecularpain.com/content/7/1/23

MOLECULAR PAIN

RESEARCH Open Access

# (-)-Pentazocine induces visceral chemical antinociception, but not thermal, mechanical, or somatic chemical antinociception, in μ-opioid receptor knockout mice

Soichiro Ide[1,2], Masabumi Minami[1], George R Uhl[3], Masamichi Satoh[4], Ichiro Sora[3,5] and Kazutaka Ikeda[2*]

## Abstract

**Background:** (-)-Pentazocine has been hypothesized to induce analgesia via the κ-opioid (KOP) receptor, although the involvement of other opioid receptor subtypes in the effects of pentazocine remains unknown. In this study, we investigated the role of the μ-opioid (MOP) receptor in thermal, mechanical, and chemical antinociception induced by (-)-pentazocine using MOP receptor knockout (MOP-KO) mice.

**Results:** (-)-Pentazocine-induced thermal antinociception, assessed by the hot-plate and tail-flick tests, was significantly reduced in heterozygous and abolished in homozygous MOP-KO mice compared with wildtype mice. The results obtained from the (-)-pentazocine-induced mechanical and somatic chemical antinociception experiments, which used the hind-paw pressure and formalin tests, were similar to the results obtained from the thermal antinociception experiments in these mice. However, (-)-pentazocine retained its ability to induce significant visceral chemical antinociception, assessed by the writhing test, in homozygous MOP-KO mice, an effect that was completely blocked by pretreatment with nor-binaltorphimine, a KOP receptor antagonist. *In vitro* binding and cyclic adenosine monophosphate assays showed that (-)-pentazocine possessed higher affinity for KOP and MOP receptors than for δ-opioid receptors.

**Conclusions:** The present study demonstrated the abolition of the thermal, mechanical, and somatic chemical antinociceptive effects of (-)-pentazocine and retention of the visceral chemical antinociceptive effects of (-)-pentazocine in MOP-KO mice. These results suggest that the MOP receptor plays a pivotal role in thermal, mechanical, and somatic chemical antinociception induced by (-)-pentazocine, whereas the KOP receptor is involved in visceral chemical antinociception induced by (-)-pentazocine.

**Keywords:** Opioid receptor Knockout mice, Pentazocine, Antinociception

## Background

The racemic compound (±)-pentazocine is used for the management of mild to moderate pain in humans. (-)-Pentazocine is known to act as an opioid analgesic, and (+)-pentazocine is a σ receptor agonist without analgesic effects. The antinociceptive effects of (-)-pentazocine are reportedly mediated by its agonist action at the κ-opioid (KOP) receptor [1]. A previous report showed that the antinociceptive effects of (-)-pentazocine were antagonized by nor-binaltorphimine (nor-BNI, a selective KOP receptor antagonist) but not by β-funaltrexamine (a selective μ-opioid [MOP] receptor antagonist) in the mouse tail-flick test [2]. However, (-)-pentazocine reportedly binds not only KOP receptors but also MOP receptors with high affinity [2] and acts as a MOP receptor partial agonist. Furthermore, the antinociceptive effects of (-)-pentazocine were antagonized by β-funaltrexamine in the mouse hot-plate test [3] and writhing test [4]. Thus, the role of the MOP receptor in the antinociceptive effects of

* Correspondence: ikeda-kz@igakuken.or.jp
[2]Research Project for Addictive Substances, Tokyo Metropolitan Institute of Medical Science, Tokyo 156-8506, Japan
Full list of author information is available at the end of the article

(-)-pentazocine remains unclear. Moreover, the most selective ligands for specific opioid receptor subtypes (e.g., β-funaltrexamine for the MOP receptor, naltrindole for the δ-opioid [DOP] receptor, and nor-BNI for the KOP receptor) possess certain affinities for other opioid receptor subtypes [5]. Thus, the precise molecular mechanisms that underlie the antinociceptive effects of (-)-pentazocine have not been clearly delineated by traditional pharmacological studies that use only selective ligands.

Developing mice that lack the MOP receptor gene has made possible the discovery of the molecular mechanisms that underlie the effects of opioids [6-9]. Both the analgesic and rewarding effects of morphine are abolished in MOP receptor knockout (MOP-KO) mice [7-9]. Buprenorphine, a nonselective opioid receptor partial agonist, exerts no analgesic effects in the tail-flick and hot-plate tests but a significant rewarding effect in the conditioned place preference paradigm in homozygous MOP-KO mice [10]. These observations are especially interesting because the distributions of DOP and KOP receptors are not apparently altered in MOP-KO mice [6,7,9]. Furthermore, butorphanol, a nonselective opioid receptor partial agonist, exerts no thermal or mechanical antinociceptive effects but exerts visceral chemical antinociceptive effects that are sensitive to nor-BNI in MOP-KO mice [11]. Although several compensatory changes might occur in KO animals, these animal models have potential utility in the investigation of the *in vivo* roles of specific proteins. Thus, the use of MOP-KO mice has provided novel theories on the molecular mechanisms that underlie the effects of opioid ligands. The present study investigated the molecular mechanisms that underlie the antinociceptive effects of (-)-pentazocine using various types of nociceptive stimuli in MOP-KO mice.

## Methods

### Animals

The present study used wildtype, heterozygous, and homozygous MOP-KO mouse littermates from heterozygous/heterozygous MOP-KO crosses on a C57BL/6J genetic background (backcrossed at least 10 generations) as previously described [8]. The experimental procedures and housing conditions were approved by the Institutional Animal Care and Use Committee, and all animal care and treatment were in accordance with our institutional animal experimentation guidelines. Naive adult (>10 weeks old) male and female mice were group housed in an animal facility maintained at 22 ± 2°C and 55 ± 5% relative humidity under a 12 h/12 h light/dark cycle with lights on at 8:00 AM and off at 8:00 PM. Food and water were available *ad libitum*.

### Drugs

(-)-Pentazocine and nor-BNI dihydrochloride were purchased from Sigma Chemical Co. (St. Louis, MO). For the *in vitro* assays, [D-Ala$^2$,*N*-MePhe$^4$,Gly-ol$^5$]enkephalin (DAMGO), a MOP-selective agonist, and [D-Pen$^2$,D-Pen$^5$]enkephalin (DPDPE), a DOP agonist, were purchased from Peninsula Laboratories Ltd. (Merseyside, UK). (+)-(5α,7α,8β)-*N*-methyl-*N*-[7-(1-pyrrolidinyl)-1-oxaspirol[4,5]dec-8-yl]benzeneacetamide (U69593), a KOP-selective agonist, was a gift from Upjohn (Kalamazoo, MI). [tyrosyl-3,5-$^3$H(N)]DAMGO (50.5 Ci/mmol), [phenyl-3,4-$^3$H]U69593 (47.5 Ci/mmol), and [tyrosyl-2,6-$^3$H(N)]DPDPE (33.0 Ci/mmol) were purchased from DuPont-New England Nuclear (Boston, MA).

### Antinociceptive tests

Thermal antinociception was evaluated using the hot-plate and tail-flick tests. Hot-plate testing was performed according to the method of Woolfe and MacDonald (1944) [12] with slight modifications. A commercially available apparatus that consisted of an acrylic resin cage (20 × 25 × 25 cm, width × length × height) and a temperature-controlled aluminum plate (Model MK-350A, Muromachi Kikai Co., Tokyo, Japan) was used for this test. Mice were placed on a 52 ± 0.2°C hot-plate, and the latencies to lick the hind-paw and jump were recorded. We selected a relatively low temperature (52° C) to examine the mild thermal antinociceptive effects of opioid partial agonists [10]. The cut-off time was 60 s. Tail-flick testing was performed according to the method of D'Amour and Smith (1941) [13] with slight modifications using a commercially available apparatus that consisted of an irradiator for heat stimulation and a photosensor for the detection of tail-flick behavior (Model MK-330A, Muromachi Kikai Co., Tokyo, Japan). The mice were loosely wrapped in a felt towel. Their tails were heated, and tail-flick latencies were automatically recorded. The cut-off time was 15 s. The tail-flick test was followed by the hot-plate test, and both tests were conducted in the same mice. Mechanical antinociception was evaluated using the hind-paw pressure test according to the method of Randall and Selitto (1957) [14] with slight modifications using a commercially available apparatus (Pressure Analgesy-Meter, Model MK-201D, Muromachi Kikai Co., Tokyo, Japan). The mice were loosely wrapped in a felt towel. Their hind-paws were gradually pressed, and hind-paw withdrawal and struggle latencies were automatically recorded. The cut-off pressure was 250 mmHg. The drug injection volume was 10 ml/kg. (-)-Pentazocine was administered at doses of 3, 7, 20, and 26 mg/kg (s.c.), for cumulative doses of 3, 10, 30, and 56 mg/kg, respectively. Tail-flick, hot-plate, and hind-paw pressure tests were conducted

20 min after each drug injection, and then the next dose of drug was injected immediately after these tests.

The hot-plate, tail-flick, and hind-paw pressure responses of each mouse in the drug-induced antinociception tests were converted to the percentage of maximal possible effect (%MPE) according to the following formula:

$$\%MPE = (postdrug\ latency - predrug\ latency) / (cut - off\ time\ or\ pressure) - predrug\ latency) \times 100\%$$

Visceral chemical antinociception was evaluated using the writhing test (Collier et al., 1968) [15]. Acetic acid (0.6% v/v, 10 ml/kg) was injected intraperitoneally (i.p.), and the mouse was placed in a large plastic cage. The intensity of nociceptive behavior was quantified by counting the total number of writhes that occurred between 0 and 15 min after the acetic acid injection. The writhing response consists of contraction of the abdominal muscles. Nociception is expressed as a writhing score during the 15 min period. (-)-Pentazocine (10 mg/kg, s.c.) or saline was administered 10 min before the acetic acid injection in a blind manner. nor-BNI (10 and 20 mg/kg, s.c.) was administered 24 h before the (-)-pentazocine injection.

Somatic chemical antinociception was evaluated using the formalin test in a blind manner as previously described [16]. Formalin (5% v/v, 20 μl) was injected into the right hind-paw (intraplantar), and the mouse was placed in a large plastic cage. The amount of time the mouse spent elevating, licking, shaking, or biting the injected paw was measured for each 5 min period during a 60 min session. Nociception was quantified using a rating scale by assigning weights to the following categories of nociceptive behavior: category 0 (weight is evenly distributed among all paws), category 1 (injected paw is lifted), category 2 (injected paw is licked, shaken, or bitten). The nociceptive score was calculated for each 5 min (300 s) period using the following formula:

$$Nociceptive\ score = \{(time\ [s]\ spent\ lifting\ the\ injected\ paw) \times 1 + (time\ [s]\ spent\ licking,\ shaking,\ or\ biting\ the\ injected\ paw) \times 2\}/300\ s.$$

(-)-Pentazocine (10 mg/kg, s.c.) or saline was administered 10 min before formalin injection (intraplantar) in a blind manner.

### Stable expression of human opioid receptors in Chinese hamster ovary cells

Chinese hamster ovary (CHO) cell lines that stably express human MOP, DOP, and KOP (MOP/CHO, DOP/CHO, and KOP/CHO, respectively) were established as previously described [10]. The $K_d$ values of [$^3$H]DAMGO binding to MOP, [$^3$H]DPDPE binding to DOP, and [$^3$H]U69593 binding to KOP were 1.7 ± 0.3 nM ($n$ = 4), 2.2 ± 0.2 nM ($n$ = 4), and 2.5 ± 0.2 nM ($n$ = 3), respectively. The $B_{max}$ estimates of receptor densities in these cell lines were 2300 ± 160, 3000 ± 270, and 5000 ± 450 fmol/mg protein, respectively.

### Radioligand binding assay

Binding assays were performed as previously described [17] with slight modifications. Expressing cells were harvested after 65 h in culture, homogenized in 50 mM Tris buffer (pH 7.4) that contained 10 mM $MgCl_2$ and 1 mM EDTA, pelleted by centrifugation for 20 min at 30000 × $g$, and resuspended in the same buffer. For the saturation binding assays, cell membrane suspensions were incubated for 60 min at 25°C with various concentrations of [$^3$H]DAMGO for the human MOP receptor, [$^3$H]DPDPE for the human DOP receptor, or [$^3$H]U69593 for the human KOP receptor. Nonspecific binding was determined in the presence of 10 mM unlabeled ligands. For the competitive binding assays, the cell membrane suspensions were incubated for 60 min at 25°C with 2 nM [$^3$H]DAMGO for the human MOP receptor, 2 nM [$^3$H]DPDPE for the human DOP receptor, or 3 nM [$^3$H]U69593 for the human KOP receptor in the presence of various concentrations of ligands. After incubation for 60 min, the membrane suspensions were rapidly filtrated, and the radioactivity of each filter was then measured by liquid scintillation counting. The $K_d$ values of the radiolabeled ligands were obtained by Scatchard analysis of the data from the saturation binding assay. For the competitive binding assay, non-linear regression analysis using a one-competition model (GraphPad Prism, GraphPad, San Diego, CA) was conducted to estimate the inhibitory concentration at 50% ($IC_{50}$). $K_i$ values were calculated from the $IC_{50}$ values obtained from the competitive binding assay using the equation $K_i = IC_{50} / (1 + [radiolabeled\ ligand]/K_d)$, where $IC_{50}$ is the concentration of unlabeled ligand that produces 50% inhibition of the specific binding of radiolabeled ligand. The binding assay results are expressed as the mean ± SEM of four independent experiments, each performed in duplicate.

### cAMP assay

3',5'-Cyclic adenosine monophosphate (cAMP) assays were performed as previously described [17] with slight modifications. Briefly, $10^5$ cells were placed into each well of a 24-well plate, grown for 24 h, washed, and incubated with 0.45 ml HEPES-buffered saline that contained 1 mM 3-isobutyl-1-methylxanthine for 10 min at 37°C. The cells were then stimulated for 10 min by the addition of 50 ml HEPES-buffered saline that contained 100 mM forskolin and 1 mM 3-isobutyl-1-methylxanthine in the presence or absence of various concentrations of opioid ligands and then disrupted by adding

0.5 ml ice-cold 10% trichloroacetic acid to each well. The concentrations of cAMP were measured by radioimmunoassay (Amersham, Buckinghamshire, UK). cAMP accumulation is expressed as a fraction of the control value obtained without the addition of opioids. Inhibition curves were generated using non-linear least-squares fit using GraphPad Prism (GraphPad, San Diego, CA). $IC_{50}$ values were calculated as the concentration of ligand that produces 50% of maximal inhibition of cAMP accumulation. The $IC_{50}$ values and maximal inhibitory effects ($I_{max}$) in the cAMP assays are expressed as mean ± SEM of four independent experiments, each performed in triplicate.

### Statistical analyses

The dose-response functions of the thermal and mechanical antinociceptive effects of (-)-pentazocine were statistically evaluated by three-way, mixed-design analysis of variance (ANOVA) with two between-subjects factors (sex and genotype) and one within-subjects factor (drug dose). Differences among genotypes were statistically evaluated by two-way, mixed-design ANOVA followed by the Bonferroni *post hoc* test. The visceral chemical antinociceptive effects of (-)-pentazocine were analyzed by one-way and two-way factorial ANOVA followed by the Bonferroni *post hoc* test. The somatic chemical antinociceptive effects of (-)-pentazocine were statistically evaluated by four-way, mixed-design ANOVA with three between-subjects factors (drug treatment, sex, and genotype) and one within-subjects factor (time). The sum of the nociceptive scores during the 1st (0-15 min) and 2nd (15-60 min) phases were statistically evaluated by one-way factorial ANOVA followed by the Bonferroni *post hoc* test. The sum of the nociceptive scores of the (-)-pentazocine-treated groups were also analyzed by two-way factorial ANOVA with two between-subjects factors (genotype and sex). Values of $p < 0.05$ were considered statistically significant.

## Results

### Thermal antinociceptive effects

The thermal antinociceptive dose-response relationships of (-)-pentazocine were analyzed in wildtype, heterozygous, and homozygous MOP-KO mice (Figure 1). (-)-Pentazocine dose-dependently induced thermal antinociceptive effects in both wildtype and heterozygous MOP-KO mice but not in homozygous MOP-KO mice. Three-way, mixed-design ANOVA revealed that the thermal antinociceptive effects of (-)-pentazocine (% MPE) were significantly different among these genotypes in both the hot-plate test (significant difference between genotypes, $F_{2,31} = 34.39$, $p < 0.001$; significant genotype × dose interaction, $F_{8,124} = 13.53$, $p < 0.001$; Figure 1A, B) and tail-flick test (significant difference between genotypes, $F_{2,31} = 76.84$, $p < 0.001$; significant genotype × dose interaction, $F_{8,124} = 18.34$, $p < 0.001$; Figure 1C, D). The thermal antinociceptive effects of (-)-pentazocine were significantly different between male and female mice in the hot-plate test (significant difference between sexes, $F_{1,31} = 8.82$, $p < 0.01$; significant sex × dose interaction, $F_{4,124} = 4.16$, $p < 0.01$; Figure 1B) but not in the tail-flick test (no significant difference between sexes, $F_{1,31} = 2.30$, $p = 0.14$; no sex × dose interaction, $F_{4,124} = 0.78$, $p = 0.54$; Figure 1D). Although the thermal antinociceptive effects of (-)-pentazocine in the tail-flick test tended to be more pronounced in male mice than in female mice, these differences were significant only in the hot-plate test.

In the hot-plate test, two-way, mixed-design ANOVA revealed that the thermal antinociceptive effects of (-)-pentazocine were significantly different among genotypes in both males ($F_{2,18} = 18.23$, $p < 0.001$) and females ($F_{2,13} = 27.05$, $p < 0.001$; Figure 1B). The thermal antinociceptive effects of (-)-pentazocine in heterozygous and homozygous MOP-KO female mice were significantly lower than in wildtype female mice ($p < 0.05$, Bonferroni *post hoc* test). By contrast, these effects only in homozygous MOP-KO male mice were significantly lower than in wildtype male mice ($p < 0.05$, Bonferroni *post hoc* test). Furthermore, two-way, mixed-design ANOVA also revealed that the thermal antinociceptive effects of (-)-pentazocine were significantly different between male and female heterozygous MOP-KO mice ($F_{1,10} = 8.31$, $p < 0.05$) but not in wildtype and homozygous MOP-KO mice.

In the tail-flick test, two-way, mixed-design ANOVA revealed that the thermal antinociceptive effects of (-)-pentazocine were significantly different among genotypes ($F_{2,34} = 78.85$, $p < 0.001$; Figure 1C, D). The thermal antinociceptive effects of (-)-pentazocine in heterozygous and homozygous MOP-KO mice were significantly lower than in wildtype mice ($p < 0.05$, Bonferroni *post hoc* test).

### Mechanical antinociceptive effects

The mechanical antinociceptive effects of (-)-pentazocine were then analyzed in wildtype, heterozygous, and homozygous MOP-KO mice (Figure 2). (-)-Pentazocine showed dose-dependent mechanical antinociceptive effects in both wildtype and heterozygous MOP-KO mice but not in homozygous MOP-KO mice. Three-way, mixed-design ANOVA revealed that the mechanical antinociceptive effects of (-)-pentazocine were significantly different among these genotypes in the hind-paw pressure test (significant difference between genotypes, $F_{2,19} = 233.2$, $p < 0.001$; significant genotype × dose

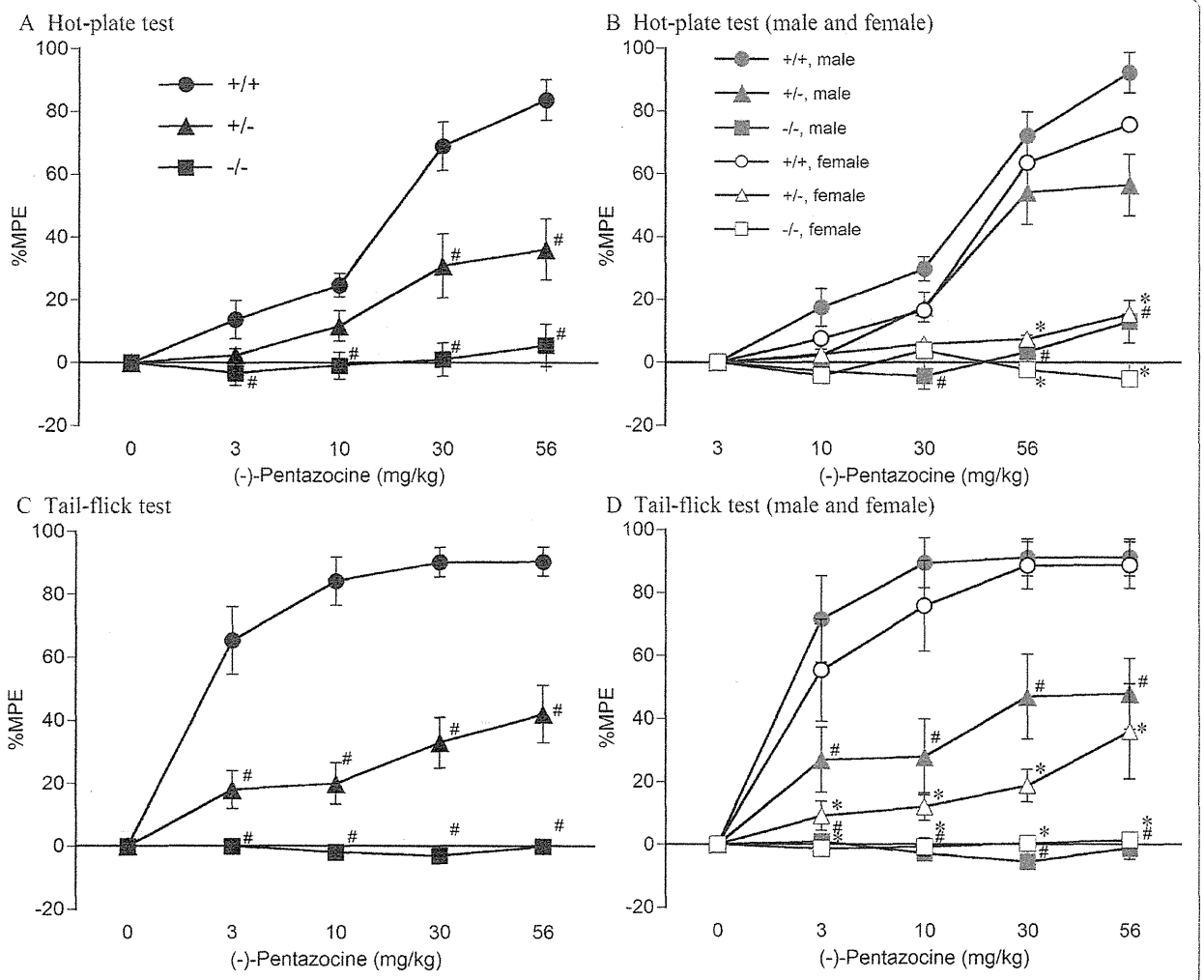


**Figure 1 Thermal antinociceptive effects of (-)-pentazocine in wildtype, heterozygous, and homozygous MOP-KO mice.** (-)-Pentazocine-induced alterations of %MPE in the hot-plate (A, B) and tail-flick (C, D) tests in wildtype (+/+; [A, C] closed circles, $n$ = 12; [B, D] gray closed circles [male, $n$ = 6], open circles [female, $n$ = 6]), heterozygous (+/-; [A, C] closed triangles, $n$ = 12; [B, D] gray closed triangles [male, $n$ = 7], open triangles [female, $n$ = 5]), and homozygous (-/-; [A, C] closed squares, $n$ = 13; [B, D] gray closed squares [male, $n$ = 8], open squares [female, $n$ = 5]) MOP-KO mice under a cumulative dose-response paradigm. (A, C) Combined data of male and female mice. $^{\#}p < 0.05$, significantly different from wildtype mice. (B, D) $^{\#}p < 0.05$, significantly different from male wildtype mice; $^{*}p < 0.05$, significantly different from female wildtype mice. Data are expressed as mean ± SEM.

interaction, $F_{8,76}$ = 38.29, $p < 0.001$; Figure 2). In contrast, these effects in the hind-paw pressure test were not significantly different between male and female mice (no significant difference between sexes, $F_{1,19}$ = 0.58, $p$ = 0.45; no sex × dose interaction, $F_{4,124}$ = 0.78, $p$ = 0.54; Figure 2B). Two-way, mixed-design ANOVA revealed that the mechanical antinociceptive effects of (-)-pentazocine were significantly different among genotypes ($F_{2,22}$ = 257.5, $p < 0.001$; Figure 2A). The mechanical antinociceptive effects of (-)-pentazocine in both heterozygous and homozygous MOP-KO mice were significantly lower than in wildtype mice ($p < 0.05$, Bonferroni *post hoc* test).

### Visceral chemical antinociceptive effects

The visceral chemical antinociceptive effects of (-)-pentazocine (10 mg/kg, s.c.) were analyzed in wildtype, heterozygous, and homozygous MOP-KO mice using the writhing test. Interestingly, (-)-pentazocine induced visceral chemical antinociceptive effects not only in wildtype and heterozygous MOP-KO mice, but also in homozygous MOP-KO mice. One-way factorial ANOVA revealed that (-)-pentazocine significantly decreased writhing (Figure 3A) in wildtype mice ($F_{1,17}$ = 128.1, $p <$ 0.001), heterozygous MOP-KO mice ($F_{1,16}$ = 125.4, $p <$ 0.001), and homozygous MOP-KO mice ($F_{1,18}$ = 87.40, $p$ < 0.001). Although no significant differences in writhing

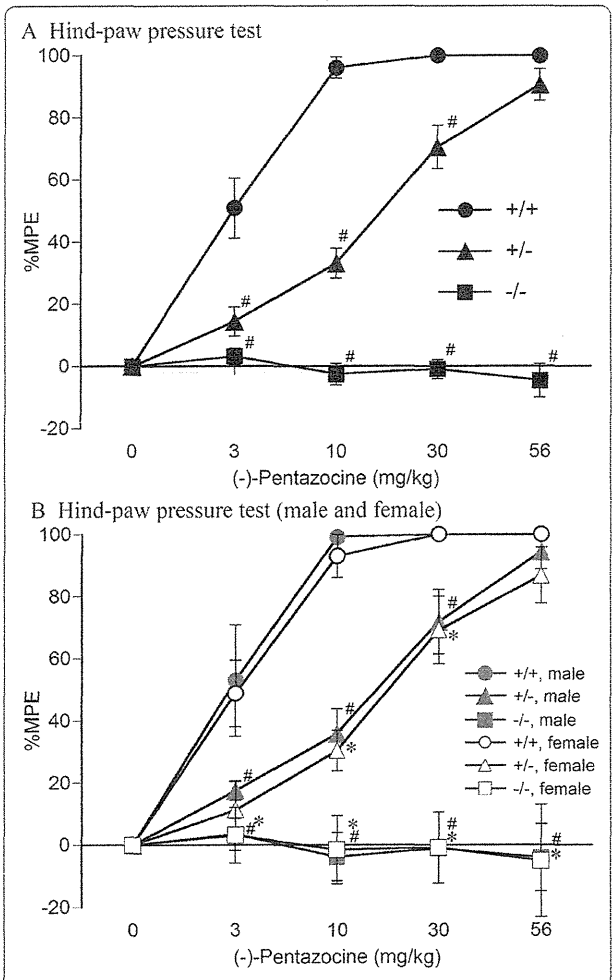


**Figure 2 Mechanical antinociceptive effects of (-)-pentazocine in wildtype, heterozygous, and homozygous MOP-KO mice.** (-)-Pentazocine-induced alterations of %MPE in the hind-paw pressure test in wildtype (+/+; [A] closed circles, $n = 8$; [B] gray closed circles [male, $n = 4$], open circles [female, $n = 4$]), heterozygous (+/-; [A] closed triangles, $n = 9$; [B] gray closed triangles [male, $n = 4$], open triangles [female, $n = 5$]), and homozygous (-/-; [A] closed squares, $n = 8$; [B] gray closed squares [male, $n = 4$], open squares [female, $n = 4$]) MOP-KO mice under a cumulative dose-response paradigm. (A) Combined data of male and female mice. $^{\#}p < 0.05$, significantly different from wildtype mice. (B) $^{\#}p < 0.05$, significantly different from male wildtype mice; $^{*}p < 0.05$, significantly different from female wildtype mice. Data are expressed as mean ± SEM.

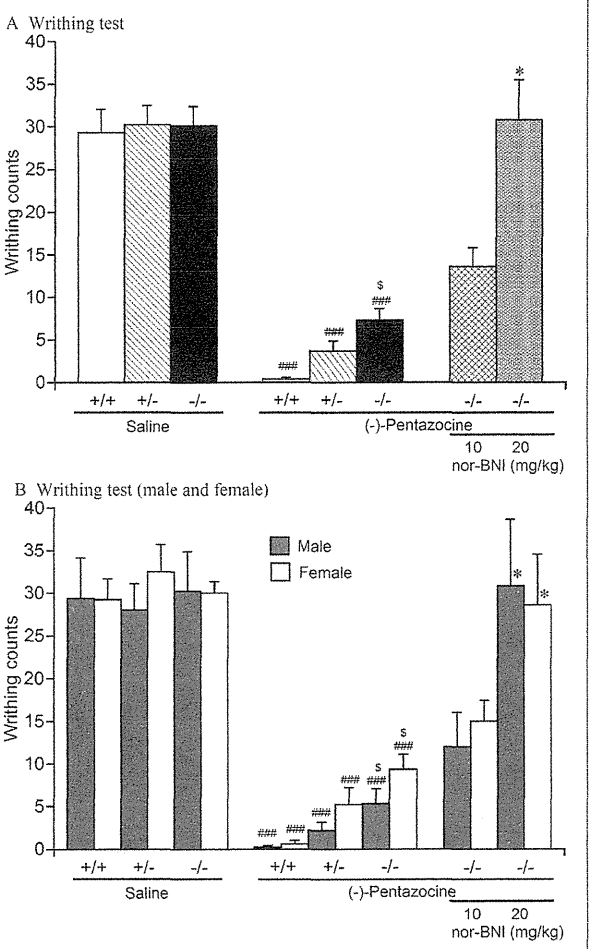


**Figure 3 Visceral chemical antinociceptive effects of (-)-pentazocine in wildtype, heterozygous, and homozygous MOP-KO mice.** Writhing counts induced by 0.6% acetic acid (i.p.) with saline pretreatment in wildtype (+/+; [A] $n = 9$; [B] male [$n = 5$], female [$n = 4$]), heterozygous (+/-; [A] $n = 8$; [B] male [$n = 8$], female [$n = 4$]), and homozygous (-/-; [A] $n = 8$; [B] male [$n = 4$], female [$n = 4$]) mice, (-)-pentazocine pretreatment (10 mg/kg, s.c.) in wildtype (+/+; [A] $n = 10$; [B] male [$n = 5$], female [$n = 5$]), heterozygous (+/-; [A] $n = 10$; [B] male [$n = 5$], female [$n = 5$]), and homozygous (-/-; [A] $n = 12$; [B] male [$n = 6$], female [$n = 6$]) MOP-KO mice, and nor-BNI (10, 20 mg/kg, s.c.) and (-)-pentazocine (10 mg/kg, s.c.) pretreatment (10 mg/kg nor-BNI: [A] $n = 11$; [B] male [$n = 5$], female [$n = 6$]; 20 mg/kg nor-BNI: [A] $n = 11$; [B] male [$n = 6$], female [$n = 5$]) in homozygous MOP-KO mice. (A) Combined data of male and female mice. (A, B) $^{\#\#\#}p < 0.001$, significantly different from saline pretreatment; $^{\$}p < 0.05$, significantly different from wildtype mice. $^{*}p < 0.05$, significantly different from (-)-pentazocine-pretreated homozygous MOP-KO mice. Data are expressed as mean ± SEM.

counts were observed in the saline-treated groups, two-way factorial ANOVA with two between-subjects factors (genotype and sex) showed significant differences in writhing counts between genotypes in the (-)-pentazocine-treated group ($F_{2,26} = 12.06$, $p < 0.001$). Furthermore, writhing counts in female mice in the (-)-pentazocine-treated group were higher than in male mice ($F_{1,26} = 4.42$, $p < 0.05$; Figure 3B). Writhing counts in (-)-pentazocine-treated homozygous MOP-KO mice were significantly higher than in both male and female wildtype mice treated with (-)-pentazocine ($p < 0.05$, Bonferroni *post hoc* test).

The remaining visceral chemical antinociceptive effects of (-)-pentazocine in homozygous MOP-KO mice

were dose-dependently antagonized by pretreatment with nor-BNI (s.c.). Two-way factorial ANOVA with two between-subjects factors (sex and nor-BNI dose) in MOP-KO mice revealed a significant difference in writhing counts between nor-BNI doses ($F_{2,28}$ = 48.07, $p$ < 0.05) but no difference between males and females. Treatment with 20 mg/kg nor-BNI in MOP-KO mice significantly antagonized the remaining visceral chemical antinociceptive effects of (-)-pentazocine ($p$ < 0.05, Bonferroni *post hoc* test).

### Somatic chemical antinociceptive effects

The somatic chemical antinociceptive effects of (-)-pentazocine (10 mg/kg, s.c.) were analyzed in wildtype, heterozygous, and homozygous MOP-KO mice using the formalin test. (-)-Pentazocine exerted somatic chemical antinociceptive effects in both wildtype and heterozygous MOP-KO mice but not in homozygous MOP-KO mice (Figure 4). Four-way, mixed-design ANOVA with three between-subjects factors (sex, genotype, and drug treatment) and one within-subjects factor (time) revealed that the nociceptive scores in the formalin test were significantly different among these genotypes (significant difference between genotypes, $F_{2,51}$ = 8.26, $p$ < 0.005; significant genotype × drug treatment interaction, $F_{2,51}$ = 11.45, $p$ < 0.001; significant genotype × time interaction, $F_{22,561}$ = 2.82, $p$ < 0.001; significant genotype × time × drug treatment interaction, $F_{22,561}$ = 2.20, $p$ < 0.005; Figure 4A). Moreover, we found a significant difference between sexes ($F_{1,51}$ = 7.57, $p$ < 0.01) and a significant sex × time interaction ($F_{11,561}$ = 2.97, $p$ < 0.005) but no sex × drug treatment interaction.

Two phases of spontaneous nociceptive behavior were analyzed (phase 1 beginning at 0 min and lasting for 15 min, and phase 2 beginning at 15 min). Therefore, the effects of (-)-pentazocine were based on the cumulative number of nociceptive scores for each phase for each mouse (Figure 4B, C). One-way factorial ANOVA revealed that (-)-pentazocine significantly decreased nociceptive scores during both phases (Figure 4B) in wildtype mice (Phase 1, $F_{1,19}$ = 16.79, $p$ < 0.005; Phase 2, $F_{1,19}$ = 99.92, $p$ < 0.001) and heterozygous MOP-KO mice (Phase 1, $F_{1,18}$ = 11.46, $p$ < 0.005; Phase 2, $F_{1,18}$ = 13.97, $p$ < 0.005) but not in homozygous MOP-KO mice. Although no significant differences in nociceptive scores were observed in the saline-treated groups, two-way factorial ANOVA with two between-subjects factors (genotype and sex) showed significant differences in nociceptive scores between the genotypes in the (-)-pentazocine-treated groups (Phase 1, $F_{2,26}$ = 16.33, $p$ < 0.001; Phase 2, $F_{2,26}$ = 21.81, $p$ < 0.001). The nociceptive scores of both the heterozygous and homozygous MOP-KO mice in the (-)-pentazocine-treated groups were significantly higher than in wildtype mice during both

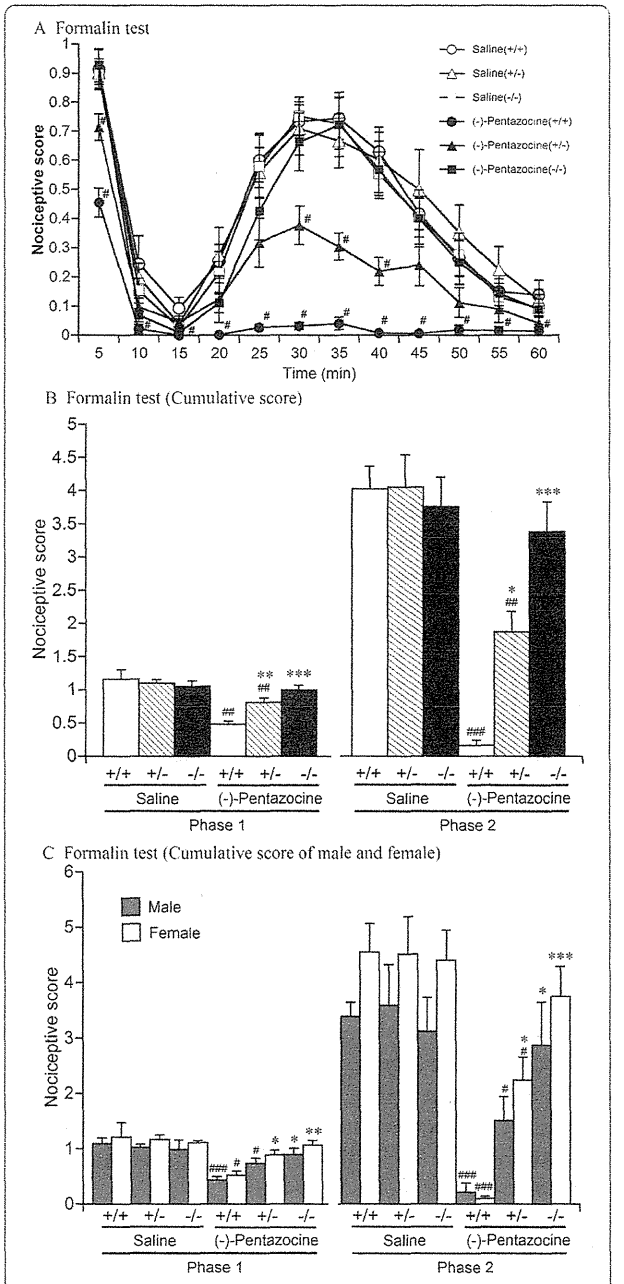


**Figure 4 Somatic chemical antinociceptive effects of (-)-pentazocine in wildtype, heterozygous, and homozygous MOP-KO mice.** Time-course of (A) and cumulative (B, C) nociceptive scores of formalin-induced nociceptive behavior with saline pretreatment in wildtype (+/+; male [$n$ = 5], female [$n$ = 6]), heterozygous (+/-; male [$n$ = 5], female [$n$ = 5]), and homozygous (-/-; male [$n$ = 5], female [$n$ = 5]) mice and (-)-pentazocine pretreatment (10 mg/kg, s.c.) in wildtype (+/+; male [$n$ = 5], female [$n$ = 5]), heterozygous (+/-; male [$n$ = 5], female [$n$ = 5]), and homozygous (-/-; male [$n$ = 5], female [$n$ = 7]) MOP-KO mice. (A, B) Combined data of male and female mice. (A-C) $^{\#}p$ < 0.05, $^{\#\#}p$ < 0.005, $^{\#\#\#}p$ < 0.001, significantly different from saline pretreatment. (B, C) $^{*}p$ < 0.05, $^{**}p$ < 0.005, $^{***}p$ < 0.001, significantly different from wildtype mice. Data are expressed as mean ± SEM.

phases ($p < 0.05$, Bonferroni *post hoc* test). By contrast, although the nociceptive scores of female mice in the (-)-pentazocine-treated groups tended to be higher than those of male mice, no significant differences were observed between sexes (Phase 1, $F_{1,26} = 3.50$, $p = 0.073$; Phase 2, $F_{1,26} = 1.59$, $p = 0.219$; Figure 4C).

### Binding characteristics

(-)-Pentazocine competition experiments using membranes prepared from MOP/CHO, DOP/CHO, and KOP/CHO cells revealed apparent binding affinities for each opioid receptor subtype (Figure 5A, Table 1). (-)-Pentazocine bound with higher affinity than morphine to membranes prepared from KOP/CHO cells. The morphine results were obtained from previous data [17] that were reanalyzed according to the present methods. Although the affinity of (-)-pentazocine for the KOP receptor was slightly higher than for the MOP receptor, (-)-pentazocine showed moderate affinity for the MOP receptor. The affinities of (-)-pentazocine for MOP and KOP receptors were higher than for DOP receptors.

### cAMP assay

The effects of (-)-pentazocine on forskolin-stimulated cAMP accumulation in MOP/CHO, DOP/CHO, and KOP/CHO cells were also tested. (-)-Pentazocine concentration-dependently suppressed forskolin-stimulated cAMP accumulation in all three cell types (Figure 5B). The $I_{max}$ values of (-)-pentazocine were lower than those of morphine for MOP/CHO cells and were the same as those of morphine for DOP/CHO and KOP/CHO cells (Table 1). The $IC_{50}$ values of (-)-pentazocine were lower than those of morphine for DOP/CHO and KOP/CHO cells (Table 1). The morphine results were obtained from previous data [17] that were reanalyzed according to the present methods. The $IC_{50}$ values of (-)-pentazocine for MOP/CHO cells were nearly the same as those for KOP/CHO cells.

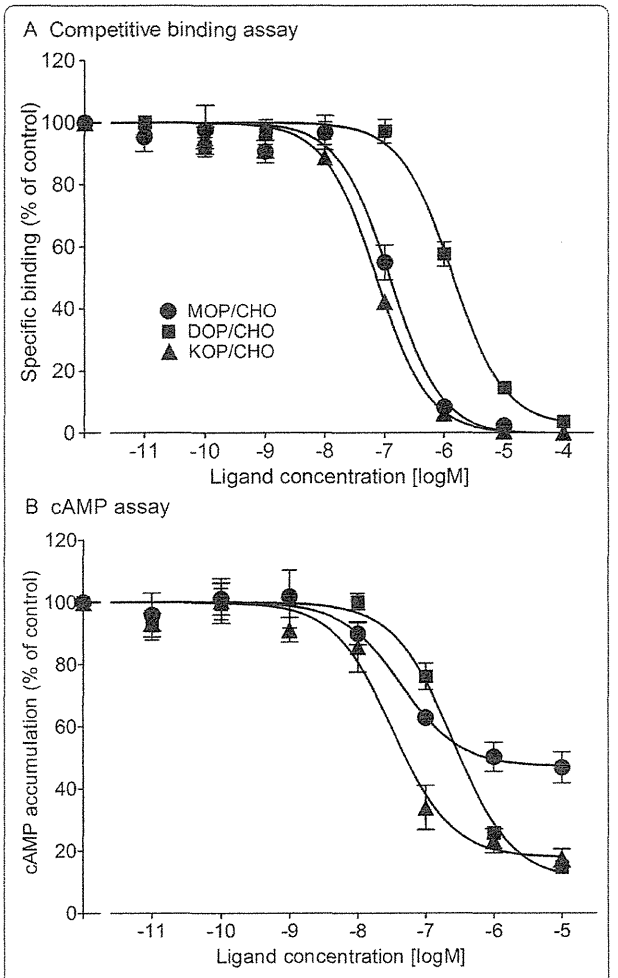


**Figure 5 Binding properties and agonist effects of (-)-pentazocine on human opioid receptor subtypes.** (A) Binding properties of (-)-pentazocine for displacement of specific binding of 2 nM [$^3$H]DAMGO, 2 nM [$^3$H]DPDPE, and 3 nM [$^3$H]U69593 to membranes of MOP/CHO cells (closed circles, $n = 4$), DOP/CHO cells (closed squares, $n = 4$), and KOP/CHO cells (closed triangles, $n = 4$), respectively. Data are expressed as mean ± SEM. (B) Agonist effects of (-)-pentazocine on forskolin-stimulated cAMP production in MOP/CHO cells (closed circles, $n = 4$), DOP/CHO cells (closed squares, $n = 4$), and KOP/CHO cells (closed triangles, $n = 4$). Intracellular cAMP levels in the cells incubated with 10 mM forskolin alone served as controls (100%). Data are expressed as mean ± SEM.

## Discussion

In the present study, the antinociceptive effects of (-)-pentazocine on various types of nociceptive stimuli were significantly reduced in heterozygous and homozygous MOP-KO mice compared with wildtype mice. The antinociceptive effects of (-)-pentazocine in these tests increased in a MOP receptor gene dose-dependent fashion. The copy numbers of the MOP receptor gene are zero in homozygous MOP-KO mice, one in heterozygous MOP-KO mice, and two in wildtype mice. These results were obtained in not only male but also female mice, although female mice may respond differently in pain tests during different phases of their estrous cycle [18]. These results suggest that the MOP receptor is the main opioid receptor involved in (-)-pentazocine-induced antinociception. The antinociceptive effects of (-)-pentazocine were previously hypothesized to be mediated by its agonist action at KOP receptors [13]. A previous report showed that the antinociceptive effects of (-)-pentazocine were antagonized by nor-BNI, a selective KOP receptor antagonist, but not by β-funaltrexamine, a selective MOP receptor antagonist, in the mouse tail-flick test [3]. However, other groups reported that the antinociceptive effects of (-)-pentazocine were

**Table 1 Binding properties and agonist effects of (-)-pentazocine and morphine on human opioid receptor subtypes**

| | MOP/CHO | DOP/CHO | KOP/CHO |
|---|---|---|---|
| Competitive binding assay | | | |
| $K_i$ value (nM) | | | |
| (-)-Pentazocine | 85.6 ± 13.3 | 641 ± 88 | 35.2 ± 2.6 |
| Morphine | 21.0 ± 3.7 | 524 ± 83 | 247 ± 13 |
| **cAMP assay** | | | |
| $IC_{50}$ (nM) | | | |
| (-)-Pentazocine | 42.8 ± 12.9 | 255 ± 46 | 39.6 ± 14.8 |
| Morphine | 25.0 ± 9.0 | 610 ± 220 | 340 ± 160 |
| $I_{max}$ (%) | | | |
| (-)-Pentazocine | 52.8 ± 3.0 | 89.3 ± 4.3 | 82.1 ± 3.7 |
| Morphine | 88.0 ± 3.1 | 83.7 ± 2.7 | 84.3 ± 3.3 |

Morphine data were obtained from a reanalysis of the data in [10].

antagonized by β-funaltrexamine in the mouse hot-plate test [3] and writhing test [4]. The discrepancy between these studies might be attributable to differences in the type of nociceptive test, strain of mice, or injection route. Furthermore, the most selective ligands for a specific subtype of opioid receptors possess certain affinities for other opioid receptor subtypes [5]. Some *in vivo* studies also demonstrated antagonist effects of nor-BNI at other opioid receptor subtypes [19,20]. Thus, the role of the MOP receptor in the antinociceptive effects of (-)-pentazocine has not been clearly evaluated by traditional pharmacological studies that only used selective ligands. The results of our *in vitro* experiments that used human MOP, DOP, and KOP receptor cDNA suggest that (-)-pentazocine induces its antinociceptive effects via the MOP receptor in humans. Although (-)-pentazocine bound to human MOP receptor with moderate affinity and showed moderate $I_{max}$ values for the MOP receptor in the cAMP assays, (-)-pentazocine had high $IC_{50}$ values for the MOP receptor in the cAMP assays, which were nearly the same as the $IC_{50}$ values for the KOP receptor and the $IC_{50}$ values of morphine for the MOP receptor. These results suggest that the MOP receptor could be involved in the antinociceptive effects of (-)-pentazocine in humans and rodents.

The antinociceptive effects of morphine, a MOP receptor agonist with low affinity for DOP and KOP receptors, are reduced in several strains of heterozygous MOP-KO mice and completely abolished in homozygous MOP-KO mice [7-9]. Furthermore, the thermal and mechanical antinociception induced by buprenorphine and butorphanol, nonselective opioid receptor partial agonists, are abolished in MOP-KO mice [10,11]. In contrast, the antinociceptive effects of morphine are not altered in mice that lack the DOP receptor [21] or in mice that lack the KOP receptor [22]. The present results, together with these previous reports, suggest that the MOP receptor may play a critical role in the analgesia induced by opioid partial agonists. MOP receptor tolerance and inactivation or individual differences in the number of MOP receptors are thus important for most of the variations in the degree of analgesia induced by opioids. Still unclear, however, is whether DOP and KOP receptors modulate the antinociceptive effects of not only (-)-pentazocine but also other opioid partial agonists. Further studies of DOP-KO, KOP-KO, and double DOP/KOP-KO mice will reveal the mechanisms that underlie these antinociceptive effects.

In contrast to thermal, mechanical, and somatic chemical antinociception, (-)-pentazocine exerted significant visceral chemical antinociception in homozygous MOP-KO mice, although the visceral chemical antinociceptive effects of (-)-pentazocine increased in a MOP receptor gene dose-dependent fashion. The residual visceral chemical antinociception induced by (-)-pentazocine was abolished by pretreatment with nor-BNI. These results indicate that both MOP and KOP receptors play dominant roles in (-)-pentazocine-induced visceral chemical antinociception, which is consistent with previous reports. The enhanced response of KOP-KO mice in the acetic acid writhing test has been previously demonstrated [22]. Furthermore, butorphanol has been shown to abolish thermal and mechanical antinociception and the nor-BNI-sensitive retention of visceral chemical antinociception in MOP-KO mice [11]. The present results, together with previous studies, suggest that both MOP and KOP receptors play important roles in visceral chemical analgesia mediated by opioid partial agonists. Furthermore, both MOP and KOP receptor-selective agonists reportedly exert significant antinociceptive effects in mice in a visceral mechanical pain model that utilizes colorectal distension [23], and peripheral KOP receptor agonists reportedly reduce visceral pain in humans [24]. The pain pathways that mediate